(2)

# NAVAL POSTGRADUATE SCHOOL

## Monterey, California






# THESIS

KEY FEATURE IDENTIFICATION FROM
IMAGE PROFILE SEGMENTS USING A
HIGH FREQUENCY SONAR

by

Barry W. Ingold

December, 1992

Thesis Advisor: Dr. Anthony J. Healey





UNCLASSIFIED

SECURITY CLASSIFICATION OF THIS PAGE

# REPORT DOCUMENTATION PAGE

| | |
|---|---|
| 1a. REPORT SECURITY CLASSIFICATION<br>UNCLASSIFIED | 1b. RESTRICTIVE MARKINGS |
| 2a. SECURITY CLASSIFICATION AUTHORITY | 3. DISTRIBUTION/AVAILABILITY OF REPORT<br>Approved for public release; distribution is unlimited. |
| 2b. DECLASSIFICATION/DOWNGRADING SCHEDULE | |
| 4. PERFORMING ORGANIZATION REPORT NUMBER(S) | 5. MONITORING ORGANIZATION REPORT NUMBER(S) |
| 6a. NAME OF PERFORMING ORGANIZATION<br>Naval Postgraduate School<br>6b. OFFICE SYMBOL (*If applicable*)<br>34 | 7a. NAME OF MONITORING ORGANIZATION<br>Naval Postgraduate School |
| 6c. ADDRESS (*City, State, and ZIP Code*)<br>Monterey, CA 93943-5000 | 7b. ADDRESS (*City, State, and ZIP Code*)<br>Monterey, CA 93943-5000 |
| 8a. NAME OF FUNDING/SPONSORING ORGANIZATION<br>8b. OFFICE SYMBOL (*If applicable*) | 9. PROCUREMENT INSTRUMENT IDENTIFICATION NUMBER |
| 8c. ADDRESS (*City, State, and ZIP Code*) | 10. SOURCE OF FUNDING NUMBERS<br>Program Element No. / Project No. / Task No. / Work Unit Accession Number |

11. TITLE (*Include Security Classification*)
KEY FEATURE IDENTIFICATION FROM IMAGE PROFILE SEGMENTS USING A HIGH FREQUENCY SONAR

12. PERSONAL AUTHOR(S) Barry W. Ingold

| 13a. TYPE OF REPORT | 13b. TIME COVERED | 14. DATE OF REPORT (*year, month, day*) | 15. PAGE COUNT |
|---|---|---|---|
| Master's Thesis | From To | 1992 December | 67 |

16. SUPPLEMENTARY NOTATION
The views expressed in this thesis are those of the author and do not reflect the official policy or position of the Department of Defense or the U.S. Government.

| 17. COSATI CODES | | | 18. SUBJECT TERMS (*continue on reverse if necessary and identify by block number*) |
|---|---|---|---|
| FIELD | GROUP | SUBGROUP | Autonomous Underwater Vehicle (AUV) |
| | | | |
| | | | |

19. ABSTRACT (*continue on reverse if necessary and identify by block number*)

Many avenues have been explored to allow recognition of underwater objects by a sensing system on an Autonomous Underwater Vehicle (AUV). In particular, this research analyzes the precision with which a Tritech ST1000 high resolution imaging sonar system allows the extraction of linear features from its perceived environment. The linear extraction algorithm, as well as acceptence criteria for individual sonar returns are developed. Test results showing the actual sonar data and the sonar's perceived environment are presented. Additionally, position of the sonar relative to the perceived image is determined based on the identification of key points in the scene.

| 20. DISTRIBUTION/AVAILABILITY OF ABSTRACT | 21. ABSTRACT SECURITY CLASSIFICATION | |
|---|---|---|
| ☒ UNCLASSIFIED/UNLIMITED ☐ SAME AS REPORT ☐ DTIC USERS | UNCLASSIFIED | |
| 22a. NAME OF RESPONSIBLE INDIVIDUAL<br>Dr. Anthony J. Healey | 22b. TELEPHONE (*Include Area code*)<br>(408) 646 - 3462 | 22c. OFFICE SYMBOL<br>ME/Hy |

DD FORM 1473, 84 MAR — 83 APR edition may be used until exhausted. All other editions are obsolete.

SECURITY CLASSIFICATION OF THIS PAGE
UNCLASSIFIED

Approved for public release; distribution is unlimited.

KEY FEATURE IDENTIFICATION FROM
IMAGE PROFILE SEGMENTS USING A
HIGH FREQUENCY SONAR

by

Barry W. Ingold
Lieutenant, United States Navy
B.S., United States Merchant Marine Academy, 1985

Submitted in partial fulfillment
of the requirements for the degree of

MASTER OF SCIENCE IN MECHANICAL ENGINEERING

from the

NAVAL POSTGRADUATE SCHOOL
December 1992

Author: Barry W. Ingold
Barry W. Ingold

Approved by:
Anthony J. Healey, Thesis Advisor

Matthew D. Kelleher, Chairman
Department of Mechanical Engineering

**ABSTRACT**

Many avenues have been explored to allow recognition of underwater objects by a sensing system on an Autonomous Underwater Vehicle (AUV). In particular, this research analyzes the precision with which a Tritech ST1000 high resolution imaging sonar system allows the extraction of linear features from its perceived environment. The linear extraction algorithm, as well as acceptence criteria for individual sonar returns are developed. Test results showing the actual sonar data and the sonar's perceived environment are presented. Additionally, position of the sonar relative to the perceived image is determined based on the identification of key points in the scene.

**TABLE OF CONTENTS**

## LIST OF FIGURES

# I. INTRODUCTION

## A. OVERVIEW

In the past decade there has been an increasing amount of research conducted in the area of Autonomous Underwater Vehicles (AUVs). This research has been aided by recent advances in computer technology and is driven by a desire to expand our capabilities in the world's oceans. The concept of an untethered independent AUV has many military as well as commercial applications. Proposed military applications include [Ref. 1]:

- Submarine support as off-hull sensors, escorts, scouts, and decoys
- Force multipliers and decoys
- Countermeasures for high speed-of-advance surface battle groups
- Open ocean and in port surveillence
- Anti-submarine warfare targets and trainers
- Mine warfare and mine countermeasures
- Special operations

Proposed commercial applications include [Refs. 2,3,4]:

- Detailed mapping of the ocean floor in support of oil exploration
- Detailed imaging of ice formations under the polar ice caps

- Marine growth removal and cleaning
- External submerged structure and pipeline inspection
- Internal cooling water tunnel inspection at a nuclear power plant

All of the aforementioned military and commercial applications require that an AUV be capable of providing reliable sensing information that can be integrated into the motion and mission planning control system architecture.

## B. NPS AUV RESEARCH PROJECT

Faculty and students from the departments of Mechanical Engineering, Computer Science, and Electrical Engineering at the Naval Postgraduate School have designed and built an unmanned untethered submersible vehicle (NPS AUV II) that is capable of operating completely submerged and unattended. The NPS AUV II is shown in Figure 1. Specific areas of research interest include:

- Vehicle stability and control
- Modeling submerged dynamic behavior
- Guidance system and autopilot design and application
- Use of ultrasonic sensors for imaging
- Design, control, and modelling of tunnel-thrusters for position keeping
- Use of Global Positioning System (GPS) receivers for navigation
- Use of neural networks for internal fault diagnostics

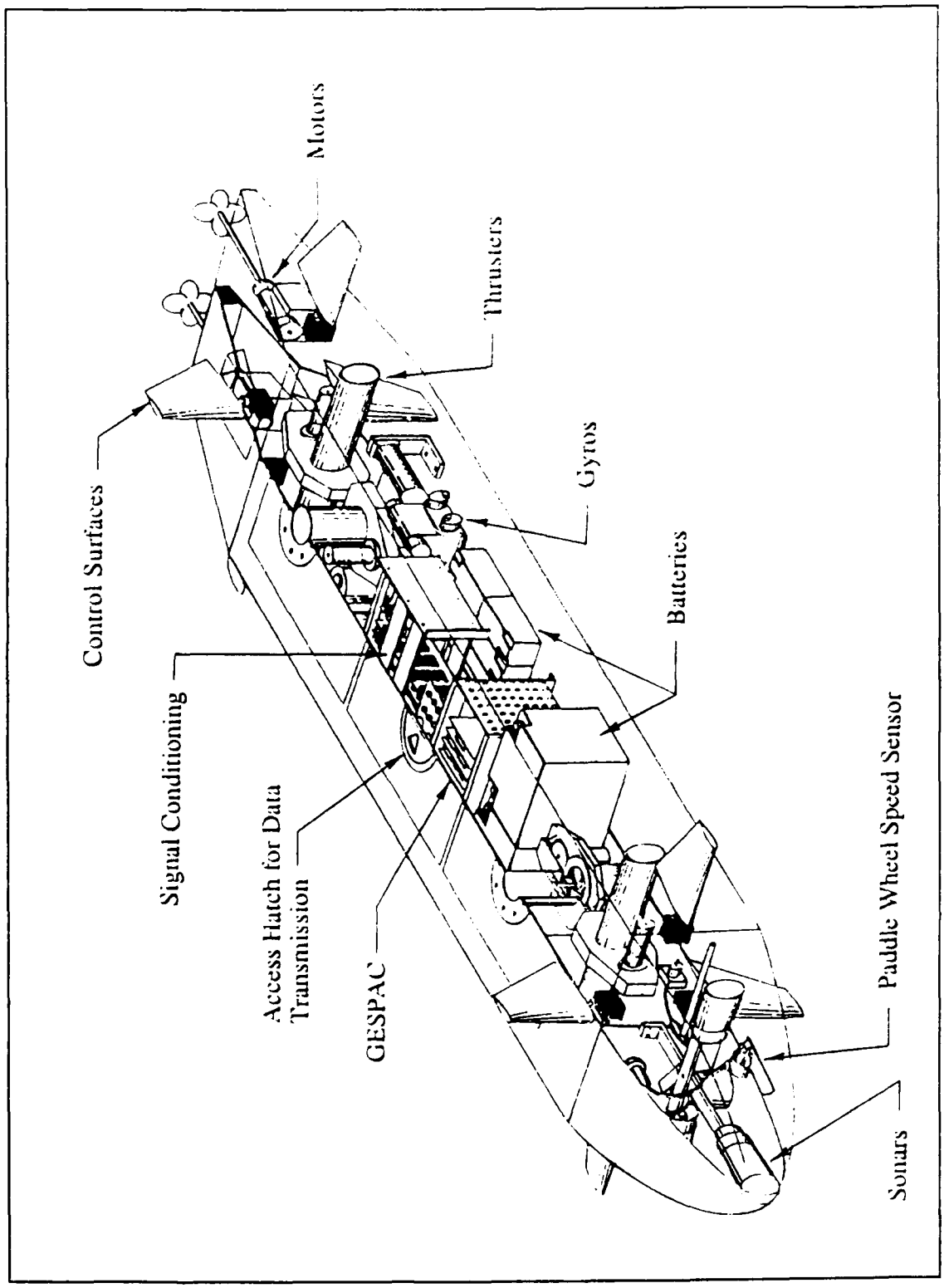


Figure 1. NPS AUV II

- Computer systems architectures for the intelligent control of AUV missions, including multiprocessor computation with vehicle dynamic and real time constraints

All of the individual topics become intimately related in their actual implimentation on NPS AUV II. This thesis will address the use of ultrasonic sensors for imaging.

## C. RELATED RESEARCH

One of the many difficulties in designing and building an AUV is to develop a sensing system that will act as its "eyes". In any intelligent robotic vehicle, it is also necessary to integrate the received information into the vehicle motion control system for the vehicle to maneuver in its perceived world. This is particularly difficult for underwater applications when considering the diffraction through the water or the possibility of turbid waters. Optical and video systems provide excellent images and are in common use with remotely operated vehicles (ROVs), but only at very limited ranges, as evidenced by the experience with the Jason ROV in the exploration of the HMS Titanic [Ref. 5]. These systems may also be rendered useless in extremely turbid water [Ref. 6]. Acoustic systems are not significantly effected by turbid water, but they provide lower resolution than video in developing a useful image.

Numerous sensing systems have been proposed, but no one system provides the end-all solution. Work with a mobile

robot on land by Elfes(1987) proposed a sonar-based mapping and navigation system that produces two-dimensional maps based on probability profiles from the sonar input to determine if areas are occupied or empty [Ref. 7]. Bahl(1990) attempted to generate three-dimensional scenes from two-dimensional sector-scanning sonar images by estimating target object height from the "length" of its acoustic shadow [Ref. 8]. Gordon(1992) employed an underwater Laser Based Synchronous Scanning System to produce high quality images [Ref. 9]. Chu, Lieberman, and Downes(1992) attempted to fine-tune the use of optical sensors in order to overcome the difficulty of the everchanging water images that are characteristic of an underwater environment [Ref. 10]. Work with underwater sonars in a mobile robot context is extremely limited. Perhaps the most detailed published information is from Russell and Lane [Refs. 11,12,13]. Additionally, Kanayama and Floyd(1991) proposed an obstacle recognition technique using a least-squares-fit algorithm for a low resolution sonar [Ref. 14]. Their algorithm uses a linear regression of the sonar data to extract linear features. It was tested using a Datasonics PSA-900 low resolution sonar system, however, the data is characterized by large noise levels.

If a vehicle is to be able to navigate within its perceived world, it must be able to identify key features automatically. This research is centered around the use of a Tritech ST1000 high resolution sonar system to extract such

key scene features, and it is of interest to determine the precision to which linear features and other shapes can be resolved and identified.

## D. OBJECTIVES

The objectives of this thesis are to:

- Determine the operating characterisitics of the Tritech ST1000 as an underwater profiling system
- Develop acceptance criteria for image feature extraction based on experimental results with the Tritech ST1000
- Evaluate the performance of the Tritech ST1000 sonar system for implimentation on the NPS AUV II
- Based on successful imaging, develop the ability to determine the position and orientation of the NPS AUV II relative to the perceived scene.

## E. THESIS ORGANIZATION

Subsequent chapters of this thesis will address the aforementioned objectives. Chapter II describes the Tritech ST1000 sonar system, including its hardware, software, and control software architecture for implementation on NPS AUV II. Chapter III describes the hovering tank at NPS that was used for testing the ST1000 sonar system. Chapter IV develops the procedure for extracting linear features from obstacles by use of a recursive least-squares-fit algorithm. Experimental results are presented in Chapter V. Finally, conclusions regarding the performance of the ST1000 sonar system and recommendations for further study are outlined in Chapter VI.

The MATLAB computer code written for this thesis is enclosed as Appendix A.

## II. TRITECH ST1000 SONAR SYSTEM

The Tritech ST1000 sonar is a high performance, high resolution compact and lightweight system designed to provide accurate measurements underwater. It was originally designed and built for use on ROVs with applications that include monitoring pipe trenches, cable laying, and sewerage pipes, as well as conducting river bed surveys and dam inspections. Another important application is the precise positioning of underwater equipment.

The basic ST1000 sonar system consists of a relatively small and lightweight sonar head that is connected via an RS-232 communications cable to a standard personnal computer(PC). The Tritech ST1000 sonar system is illustrated in Figure 2. The PC allows for a video display as well as complete control of the sonar head. The thrust of this sonar imaging research is to be able to "cut the cable" and integrate the ST1000 sonar system into the motion control and autopilot functions of the NPS AUV II.

### A. ST1000 HARDWARE

The size and weight of the ST1000 sonar head make it ideally suited for use on NPS AUV II. The sonar head is 74mm (approximately 3 inches) in diameter and 225mm (approximately

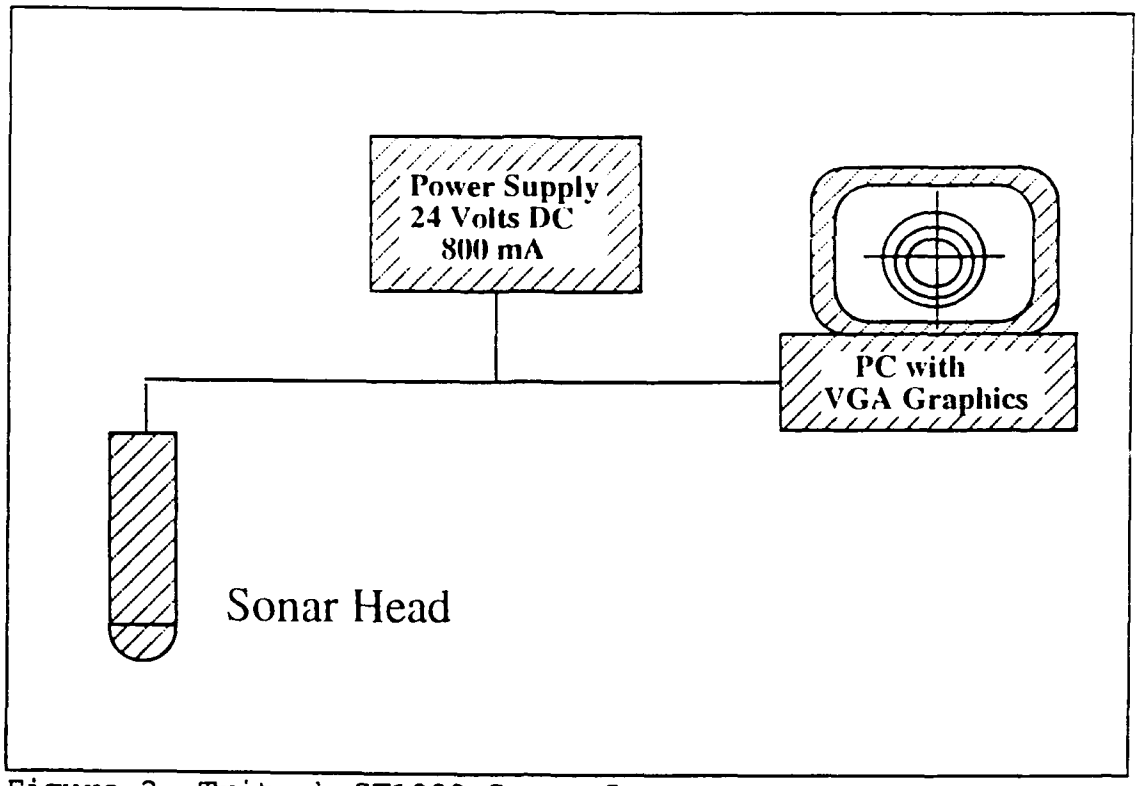

Figure 2. Tritech ST1000 Sonar System

9 inches) long. It weighs 2.43 pounds in air and 1.42 pounds in water. The ST1000 sonar head is shown in Figure 3. The sonar head is constructed of aluminum alloy HE-30 Ni/Al bronze with a hard anodised finish, and has a depth rating in excess of 4000 feet. The sonar head is powered by 24-28 VDC at 800 mA and has a nominal operating frequency of 1 MHz. While the 1 MHz operating frequency makes the ST1000 sonar very accurate, it also limits its range to 100 meters due to the effects of absorption and scattering [Ref. 15]. The sonar head generates a 1 degree conical beam which is mechanically

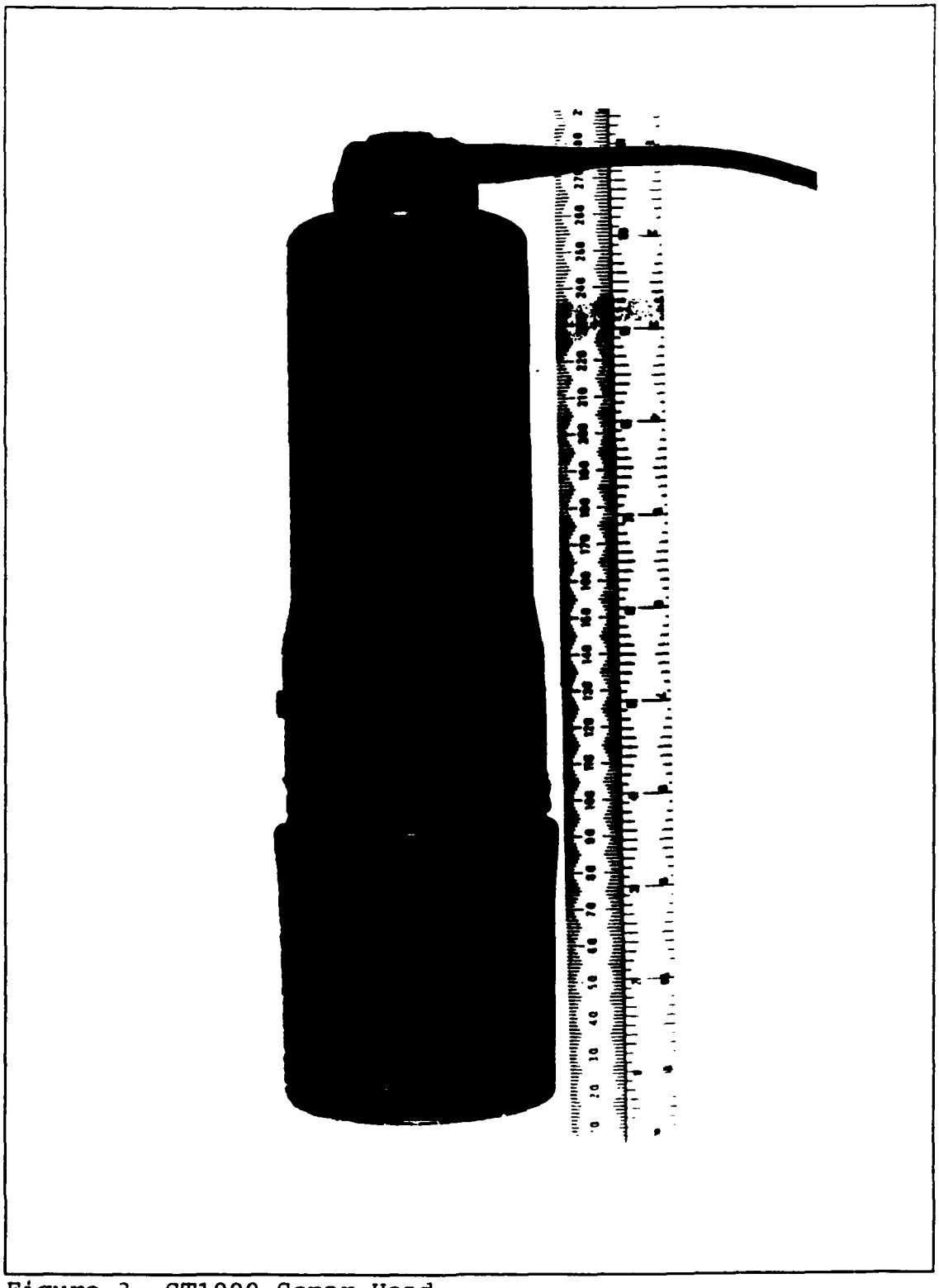

Figure 3. ST1000 Sonar Head

steered through 360 degree continuous sweeps by a stepper motor. The stepper motor is equipped with high, medium, andlow resolution modes of operation which provide step angles of 0.9, 1.8, and 3.6 degrees, respectively. Thus, while in the high resolution mode, the sweep rate of the sonar beam is slow compared to the sweep rate in the low resolution mode.

The sonar head can be mounted vertically in order to provide a horizontal sweep, or it can be mounted horizontally in order to provide a vertical sweep. The 1 degree conical beam limits the cross axis range of the sonar. At a range of 6 meters, the sonar will only ensonify a region 10.5 cm in diameter and at 50 meters the ensonified region is only 87.3 cm in diameter, (Figure 4). This severely limits the search capability of the ST1000, but improves its ability for precise positioning while in the profiling mode.

## B. ST1000 SOFTWARE

The software provided with the ST1000 sonar system is designed to be run on an IBM-PC compatible computer with VGA graphics capabilities. Control functions provided at the PC include gain, thresholding, scan direction, scan width, range, and resolution. Gain adjusts the power output of the sonar head. Increasing the gain generates stronger returns. However, a higher gain also increases the amount of unwanted noise returns. Thresholding provides a video display control to not show weak returns. All returns are processed by the

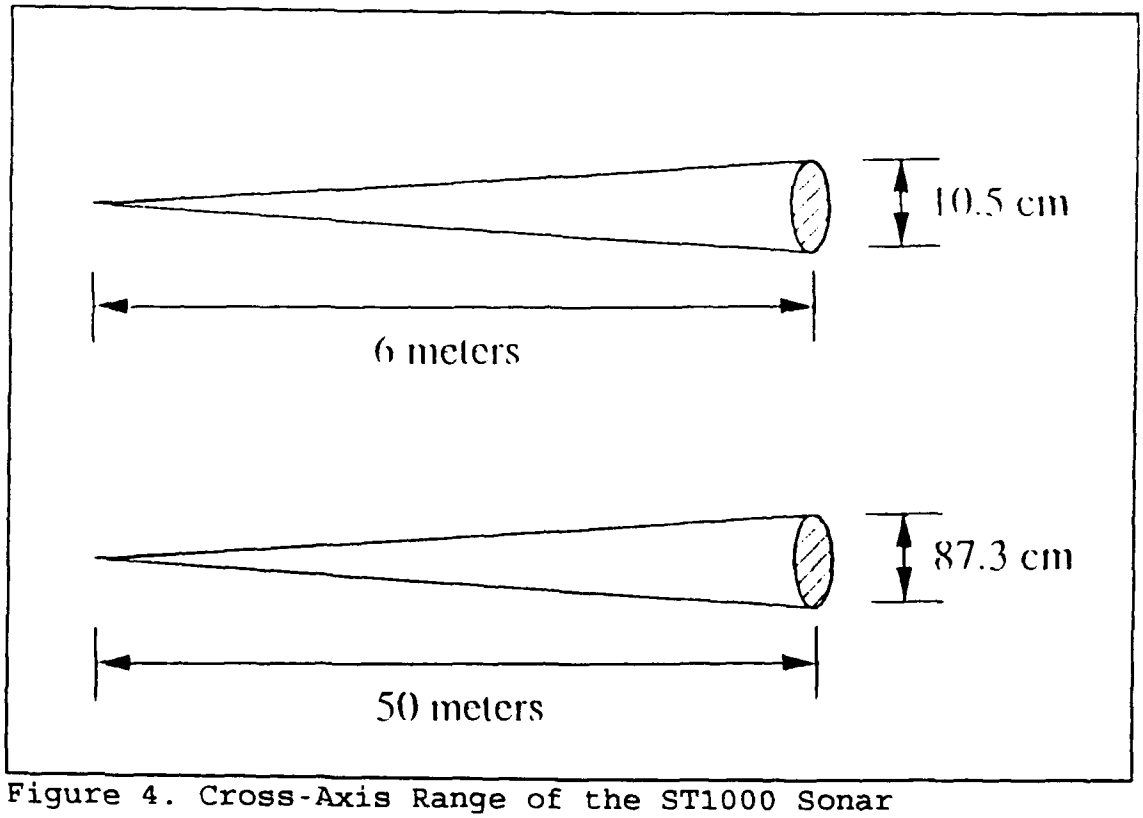

Figure 4. Cross-Axis Range of the ST1000 Sonar

system, but weak returns below the threshold level are not shown on the video display. Scan direction can be set to either clockwise or counterclockwise. Scan width can be used to set the sonar to only sweep over a designated sector of interest.

### 1. Range Processing

The ST1000 sonar system has two modes of operation; scanning and profiling.

#### *a. Scanning Mode*

In the scanning mode the ST1000 sonar system can operate at ranges of 6, 10, 20, 25, 30, 50, 75, and 100

meters. At each stepper motor bearing, the ST1000 sonar subdivides the range into 64 equally spaced range bins. This produces a range resolution of 0.094 meters when operating at a six meter range scale, and 1.56 meters when operating at a 100 meter range scale. While these resolutions are default values, software processing can reduce them by a factor of two if needed.

Each range bin is subdivided into two four bit numbers. The first four bit number represents the bin number and hence the range. The second four bit number represents the intensity of the return associated with that range. Intensity levels vary from one to 15, one being extremely weak and 15 being very strong. When using a video display, the intensities are represented by a spectrum of colors.

***b. Profiling Mode***

In the profiling mode, the ST1000 sonar emits a pulse at each stepper motor bearing and then listens for a return, computing the time to the first return. It is considered to be a strong return and is assigned an intensity of 15. This feature leads to some spurious returns, but with the gain properly adjusted, it does not significantly degrade the operation of the system. The elapsed time is converted to a range in millimeters and is saved as a 16 bit number. In this mode, the ST1000 sonar system has a theoretical range resolution of 0.76 mm based on a maximum range digitized to 16

bits. The return is also plotted as a dot on the video output.

## C. VEHICLE CONTROL SOFTWARE ARCHITECTURE RELATIVE TO SCENE PERCEPTION

A brief summary of the NPS AUV II software architecture is provided here to describe where the sonar management and signal processing is accomplished relative to other control functions in the vehicle. The software architecture on NPS AUV II is based on a rational behavior model [Ref. 16] and is subdivided into three levels: strategic, tactical, and execution. A simplistic representation of the rational behavior model is illustrated in Figure 5.

### 1. Strategic Level

The strategic level contains the mission doctrine which includes a concise operational plan specifying top-level goals. The strategic level contains no random access memory and can only provide strategic, high level commands to the tactical level.

### 2. Tactical Level

The tactical level provides coordination and translation between commands and action, and is shown in Figure 6. The tactical level also maintains vehicle status and the world model, as well as performing replanning when required. The sonar imaging algorithm developed in this

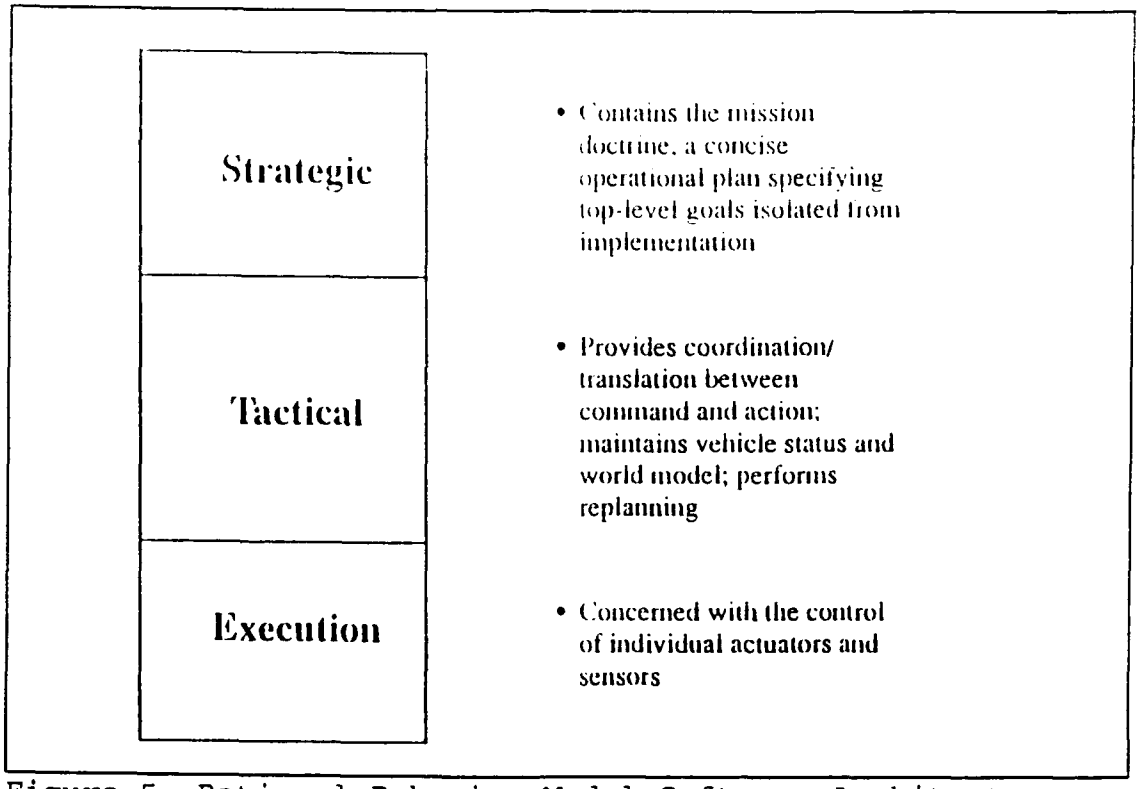

Figure 5. Rational Behavior Model Software Architecture

thesis will be employed in the tactical level of the NPS AUV II software hierarchy; specifically, in the sonar control block.

### 3. Execution Level

The execution level is concerned with the control of individual actuators and sensors. The ST1000 sonar head will be controlled via commands from the execution level with parameters as set by tactical level set points that result from scene interpretation computations.

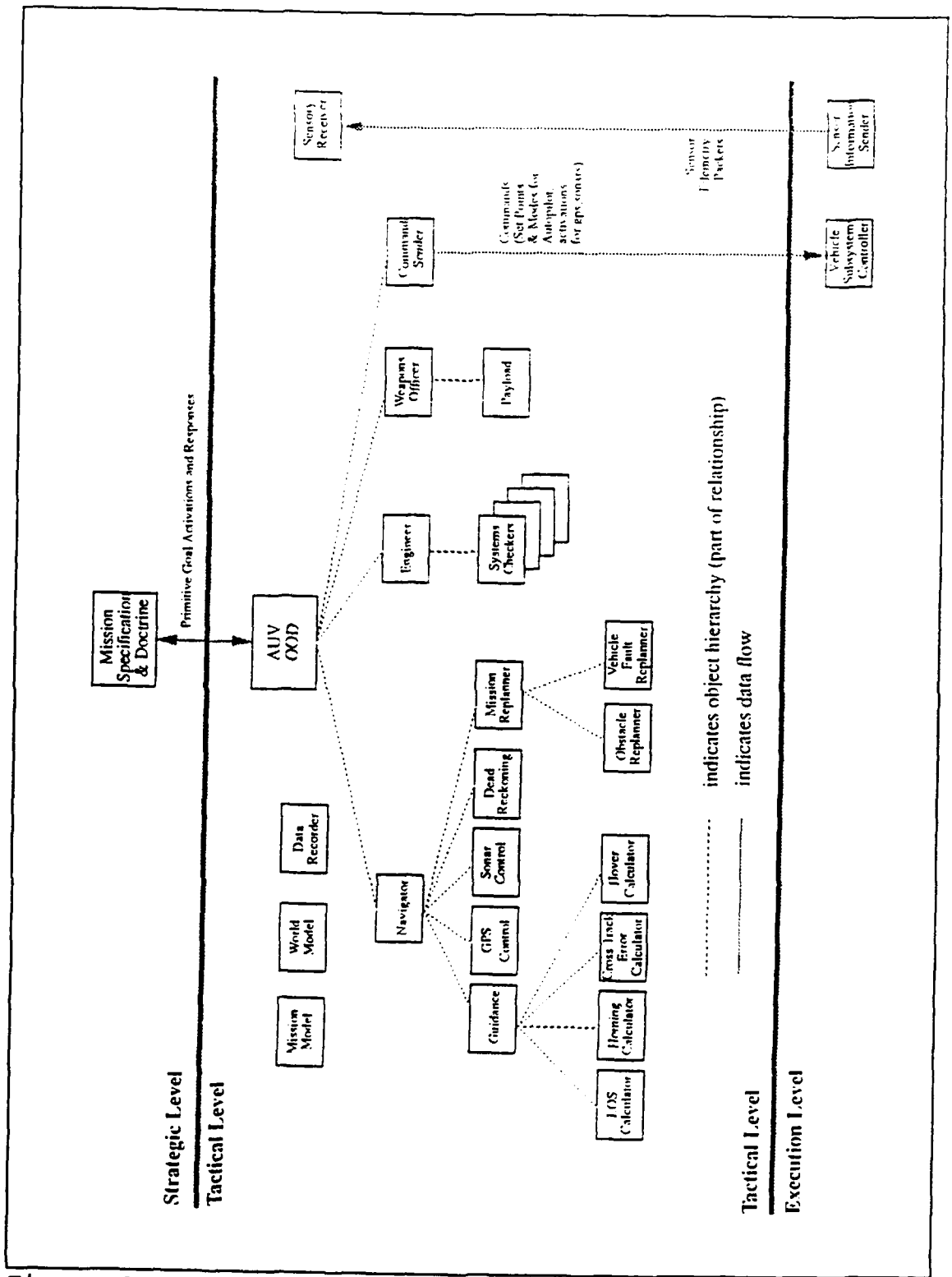


Figure 6. Tactical Level Object Hierarchy

# III. EXPERIMENTAL SETUP

## A. OVERVIEW

The ST1000 sonar system was tested in the NPS AUV II hovering tank. The hovering tank was built to test the NPS AUV II in the hover mode using tunnel thrusters, but it also provides an excellent facility for testing sonar systems. The hovering tank measures 6.096 X 6.096 meters (20 X 20 feet) and is approximately 2 meters deep. Two open ended aluminum cylinders that measure 0.30 meters in diameter were placed in the tank to act as sonar targets. One cylinder that measured 0.48 meters in length was placed on end and the other cylinder which measured 1.01 meters in length was placed on its side. Figure 7 shows the configuration of the hovering tank.

The ST1000 sonar head was suspended in the tank from a styrofoam float; low enough to ensure that the target cylinders were in the 1 degree conical beam of the sonar.

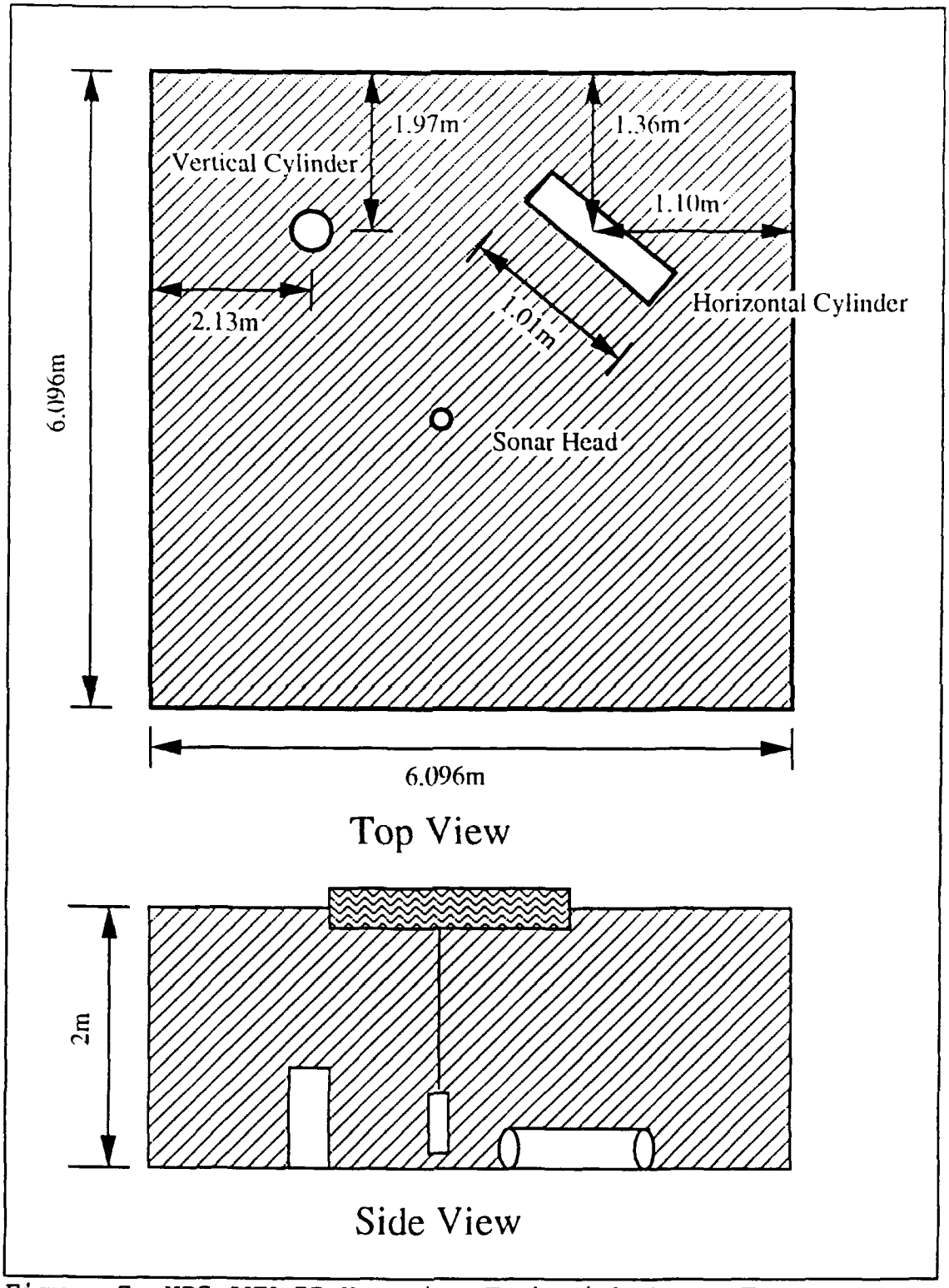


Figure 7. NPS AUV II Hovering Tank with Sonar Targets

## B. HOVERING TANK COORDINATE SYSTEM

A standardized coordinate system was defined by Brutzman(1992) [Ref. 17] in order to maintain conformity throughout the NPS AUV research project between computer simulation models, experimental data files, and computer graphics codes. This coordinate system has been adapted to the hovering tank. The advantages of this coordinate system are as follows:

- All coordinates are positive and in units of meters
- Surface depth z equals zero with increasing depth corresponding to increasing z
- NPS AUV data files coordinates become standardized for readability and future reference
- Vehicle position and posture terminology are standardized
- Right-hand rule relationships between all three axes are maintained
- Compatibility with vehicle coordinate system and Euler angle definitions
- Vehicle headings and sonar bearings are measured in a clockwise direction as are conventional compass headings
- This coordinate system simultaneously combines Cartesian coordinate plane charcteristics, Euler angles and a right-hand rule; features that are not possible with any other spatial representation

The disadvantage of this coordinate system is:

- Similarity to a Cartesian plane used in computer graphics is only evident from a perspective looking up to the tank surface from the bottom, thus axis orientations may initially be counterintuitive

The coordinate system is shown in Figure 8.

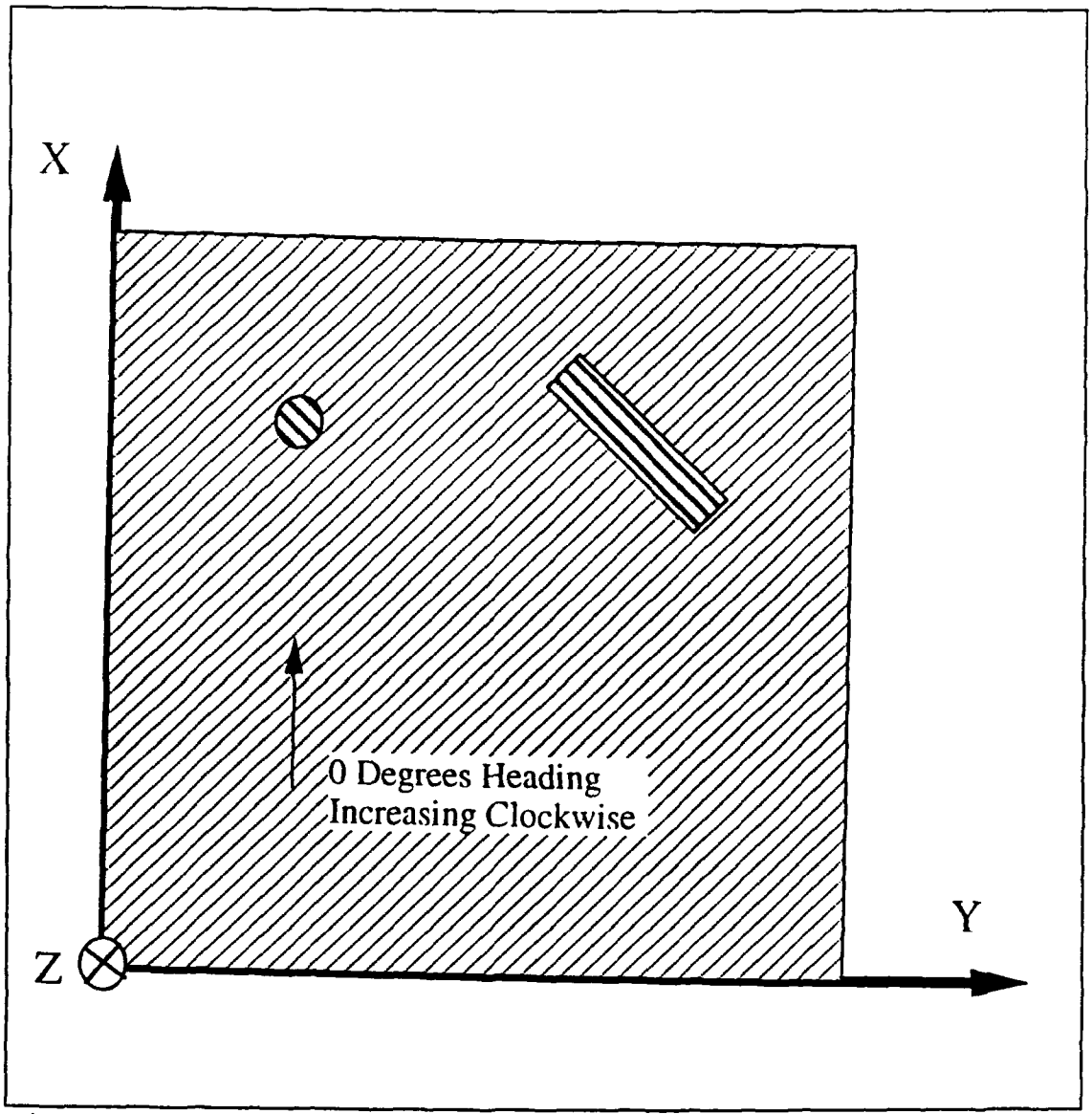


Figure 8. Hovering Tank Coordinate System

# IV. LINEAR FEATURE EXTRACTION

Regression analysis is used in a wide variety of applications to develop a linear approximation for sets of discrete data points. The particular application of interest here is the extraction of linear features from data points generated by sonar returns. This method was originally developed by Roberts(1964) [Ref. 18] for dealing with video images, and later used by Kanayama and Naguchi(1989) for sonar returns in air as tested on the land-based mobile robot Yamabico-11 [Ref. 19]. Later, Kanayama and Floyd(1991) adapted the method for an underwater low resolution sonar application on NPS AUV II [Ref. 14]. This research analyzes the precision with which a Tritech high resolution profiling sonar can extract linear features. Once linear features have been identified, vehicle position and orientation relative to the perceived scene can then be determined.

## A. COORDINATE SYSTEM TRANSFORMATION

The global position of an object can be determined from the global position of the vehicle plus the position of the object relative to the vehicle. The relative position of an object to the vehicle in the body fixed frame is determined by

the sonar and expressed in terms of a range($R$) and a bearing(B). The position of the vehicle is determined as a dead reckoning (DR) position ($x_{dr}$, $y_{dr}$) and the vehicle heading ($\Psi$) in the global frame is provided by a heading gyro. It follows that the vector addition of the vehicle position and the relative position of the object to the vehicle results in the position of the object ($x_i$, $y_i$) in the global reference frame. Conversely, if the position of an object is known, the position and orientation of the vehicle relative to the object can be determined. Figure 9 depicts this coordinate system transformation.

## B. LINEAR REGRESSION PRINCIPLES

The extraction of a linear feature from a set of data points is accomplished using a least squares fit method. Details of the definitions used in this method appeared in References 13 and 18, but are provided in order to maintain continuity for the reader. Based on valid sonar returns, the ST1000 profiling sonar generates $n$ data points in a body fixed frame in terms of range ($R$) and bearing (B). These data points are easily transformed to ($x_i$, $y_i$) points in the body fixed frame by

$$x_i = (R)\cos(\mathbf{B}) \tag{4.1}$$

and

$$y_i = (R)\sin(B) \tag{4.2}$$

resulting in a set $P$ of positions whereby

$$P = \langle (x_i, y_i) \mid i=1, \ldots, n \rangle \tag{4.3}$$

The moments of $P$ are defined as

$$m_{jk} = \sum_{i=1}^{n} x^j y^k \quad (0 \le j,\ k \le 2,\ j+k \le 2) \tag{4.4}$$

Notice that $m_{00} = n$. The centroid of $P$ is given by

$$C \equiv \left(\frac{m_{10}}{m_{00}}, \frac{m_{01}}{m_{00}}\right) \equiv (\mu_x, \mu_y) \tag{4.5}$$

The secondary moments around the centroid are given by

$$M_{20} \equiv \sum_{i=1}^{n} (x_i - \mu_x)^2 = m_{20} - \left(\frac{m_{10}^2}{m_{00}}\right) \tag{4.6}$$

$$M_{11} \equiv \sum_{i=1}^{n} (x_i - \mu_x)(y_i - \mu_y) = m_{11} - \left(\frac{m_{10} m_{01}}{m_{00}}\right) \tag{4.7}$$

$$M_{02} \equiv \sum_{i=1}^{n} (y_i - \mu_y)^2 = m_{02} - \left(\frac{m_{01}^2}{m_{00}}\right) \tag{4.8}$$

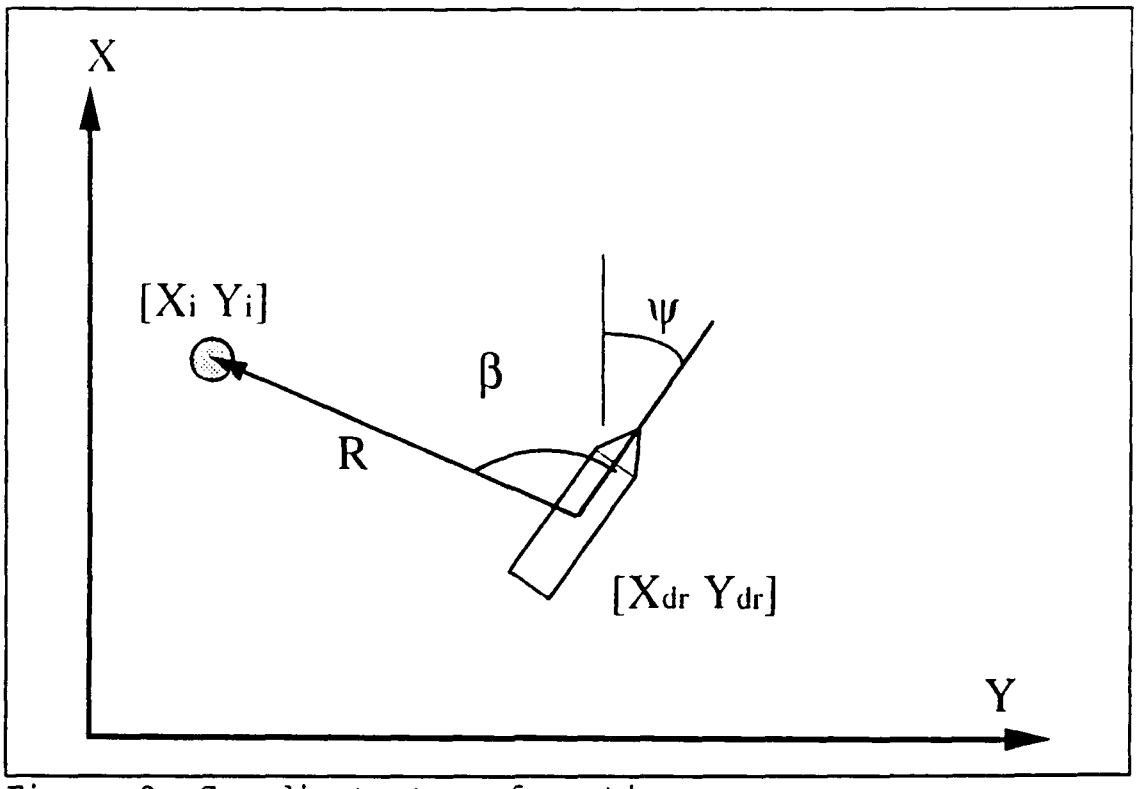

Figure 9. Coordinate transformation

The line generated by the linear regression analysis will be parametrically represented by the constants $r$ and $\alpha$ such that $r$ is the distance normal to the line and $\alpha$ is the orientation of the line. (Figure 10) A point $P_i=(x_i,y_i)$ lies on the line if it satisfies the equation

$$r = x_i\cos\alpha + y_i\sin\alpha \qquad (4.9)$$

This parametric representation of a line was chosen such that lines perpendicular to the X-axis can be represented. The point-slope method, where y = mx + b, is incapable of representing such a case (m = ∞, b is undefined). The

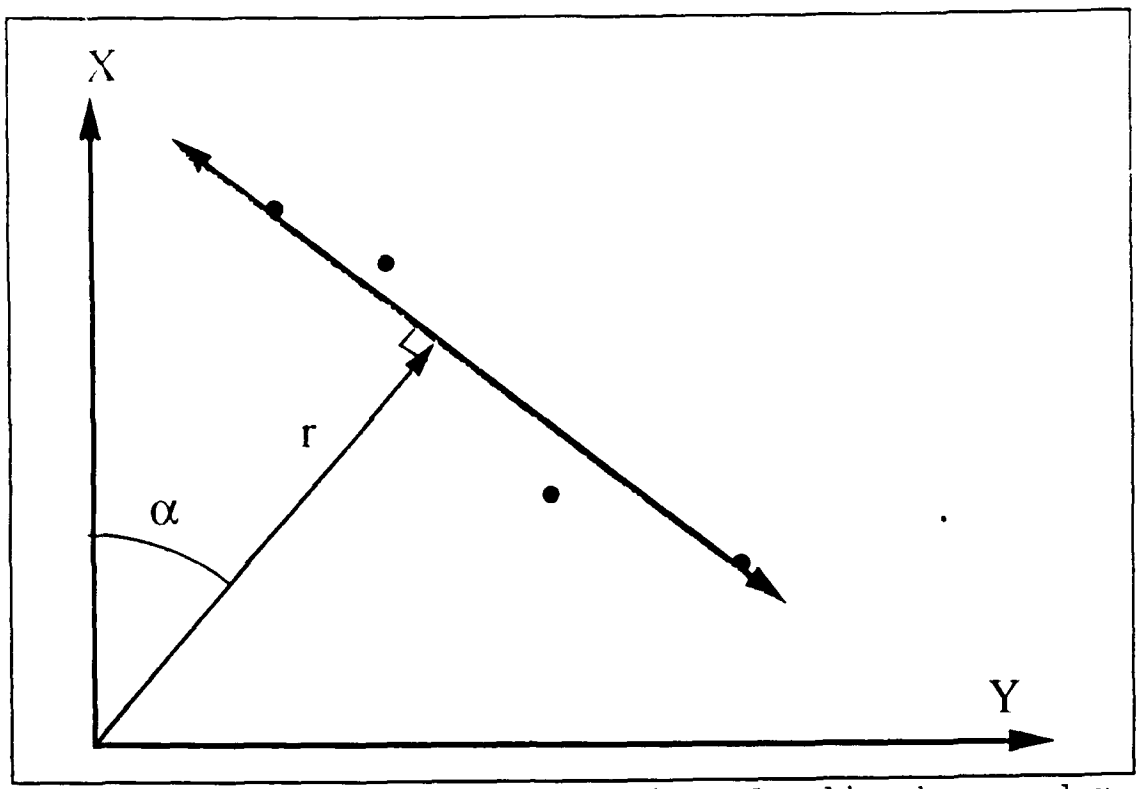

Figure 10. Parametric representation of a line by $r$ and $\alpha$

residual of a point $P_i=(x_i,y_i)$ is the perpendicular distance between the point and the parametric representation of the line such that

$$Residual = x_i\cos\alpha + y_i\sin\alpha - r \qquad (4.10)$$

Therefore, the sum of the squares of all the residuals is

$$S = \sum_{i=1}^{n} (r - x_i\cos\alpha - y_i\sin\alpha)^2 \qquad (4.11)$$

The line which best fits the sets of points will minimize S.

Thus, the optimum line $(r,\alpha)$ must satisfy

$$\frac{\partial S}{\partial r} = \frac{\partial S}{\partial \alpha} = 0 \tag{4.12}$$

Thus,

$$\begin{aligned} \frac{\partial S}{\partial r} &= 2 \sum_{i=1}^{n} (r - x_i \cos\alpha - y_i \sin\alpha) \\ &= 2 (r \sum_{i=1}^{n} 1 - (\sum_{i=1}^{n} x_i) \cos\alpha - (\sum_{i=1}^{n} y_i) \sin\alpha) \\ &= 2 (r m_{00} - m_{10} \cos\alpha - m_{01} \sin\alpha) = 0 \end{aligned} \tag{4.13}$$

and

$$\begin{aligned} r &= \frac{m_{10}}{m_{00}} \cos\alpha + \frac{m_{01}}{m_{00}} \sin\alpha \\ &= \mu_x \cos\alpha + \mu_y \sin\alpha \end{aligned} \tag{4.14}$$

where $r$ may be negative. Substituting for $r$ in (4.11) by (4.14)

$$S = \sum_{i=1}^{n} ((x_i - \mu_x) \cos\alpha + (y_i - \mu_y) \sin\alpha)^2 \tag{4.15}$$

Finally,

$$\frac{\partial S}{\partial \alpha} = 2\sum_{i=1}^{n}\left((x_i-\mu_x)\cos\alpha+(y_i-\mu_y)\sin\alpha\right)*$$
$$\left(-(x_i-\mu_x)\sin\alpha+(y_i-\mu_y)\cos\alpha\right)$$
$$= 2\sum_{i=1}^{n}\left((y_i-\mu_y)^2-(x_i-\mu_x)^2\right)\sin\alpha\cos\alpha + \qquad (4.16)$$
$$2\sum_{i=1}^{N}(x_i-\mu_x)(y_i-\mu_y)(\cos^2\alpha-\sin^2\alpha)$$
$$= (M_{02}-M_{20})\sin 2\alpha - 2M_{11}\cos 2\alpha = 0$$

Therefore

$$\alpha = \frac{arctan2(-2M_{11}, M_{02}-M_{20})}{2} \qquad (4.17)$$

The solutions for the line parameters generated by the least squares fit are given by (4.14) and (4.17).

To develop a "goodness of fit" criteria to be used to reject outliers, we now define the *equivalent ellipse of inertia* for the *n* data points generated by the sonar as the ellipse that has the same moments around its center of gravity. Thus $M_{major}$ and $M_{minor}$ are moments about the major and minor axes respectively.

$$M_{major} = \frac{(M_{20}+M_{02})}{2} + \sqrt{\frac{(M_{02}-M_{20})^2}{4}+M_{11}^2} \qquad (4.18)$$

$$M_{minor} = \frac{(M_{20}+M_{02})}{2} - \sqrt{\frac{(M_{02}-M_{20})^2}{4} + M_{11}^2} \qquad (4.19)$$

This leads to definition of the *major diameter* along the major axes as

$$d_{major} = 4\sqrt{\frac{M_{major}}{m_{00}}} \qquad (4.20)$$

and the *minor diameter* along the minor axes as

$$d_{minor} = 4\sqrt{\frac{M_{minor}}{m_{00}}} \qquad (4.21)$$

(Figure 11) Finally, the *ellipse thinness ratio* ($\rho$) is the ratio minor and major diameters

$$\rho = \frac{d_{minor}}{d_{major}} \qquad (4.22)$$

As $\rho$ tends toward zero, the ellipse is very thin and approximates a line. Conversely, as $\rho$ tends towards 1, the ellipse degrades to a circle representing a thick line or a "blob" of points. The thinness ratio provides an additional measure of linearity of a set of data points.

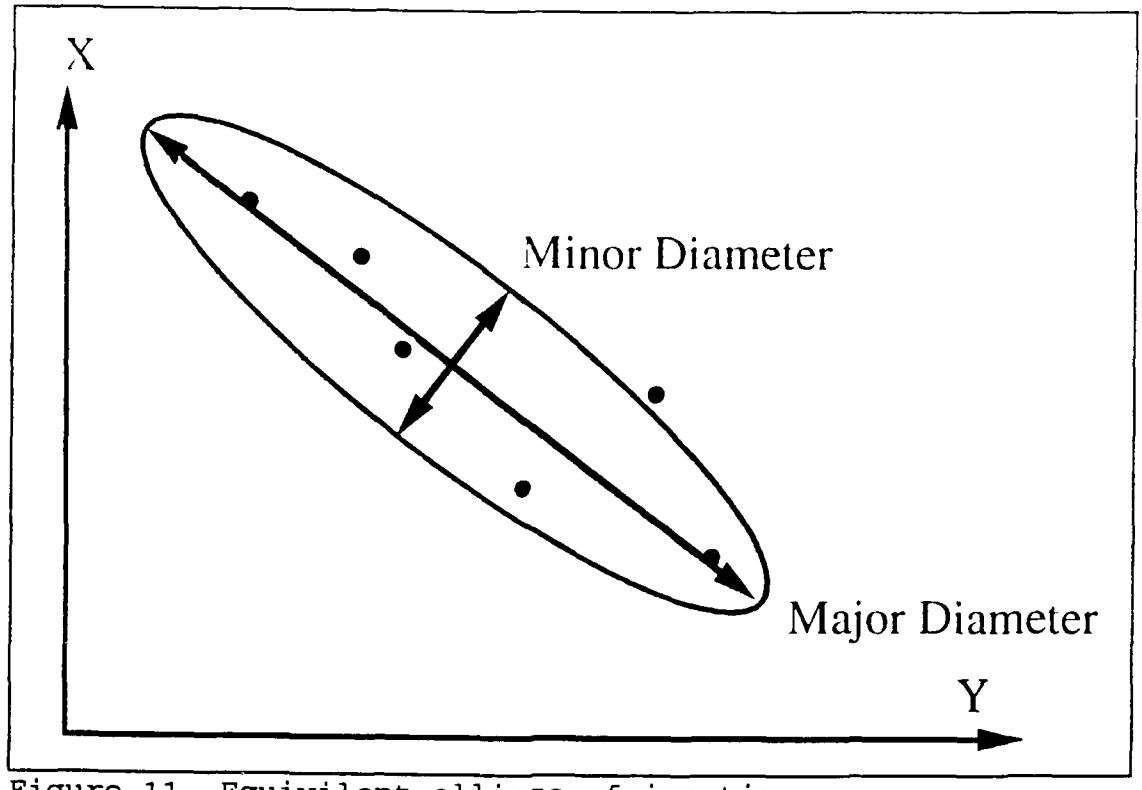

Figure 11. Equivilent ellipse of inertia

## C. LINE SEGMENTATION

Linear features are extracted from the sonar data using the linear regression method presented above. It has been found that six data points are required to initiate a line segment and determine its $r$, $\alpha$, and $\rho$. To check the validity of the next return, the expected range at the next point is predicted using the current estimates of $r$ and $\alpha$. The actual range at the next stepper motor bearing is then compared with this estimate to produce a residual error. If the new range falls within 150% of the minor diameter, corrected for angular offset at that bearing (Figure 12), then the data point is

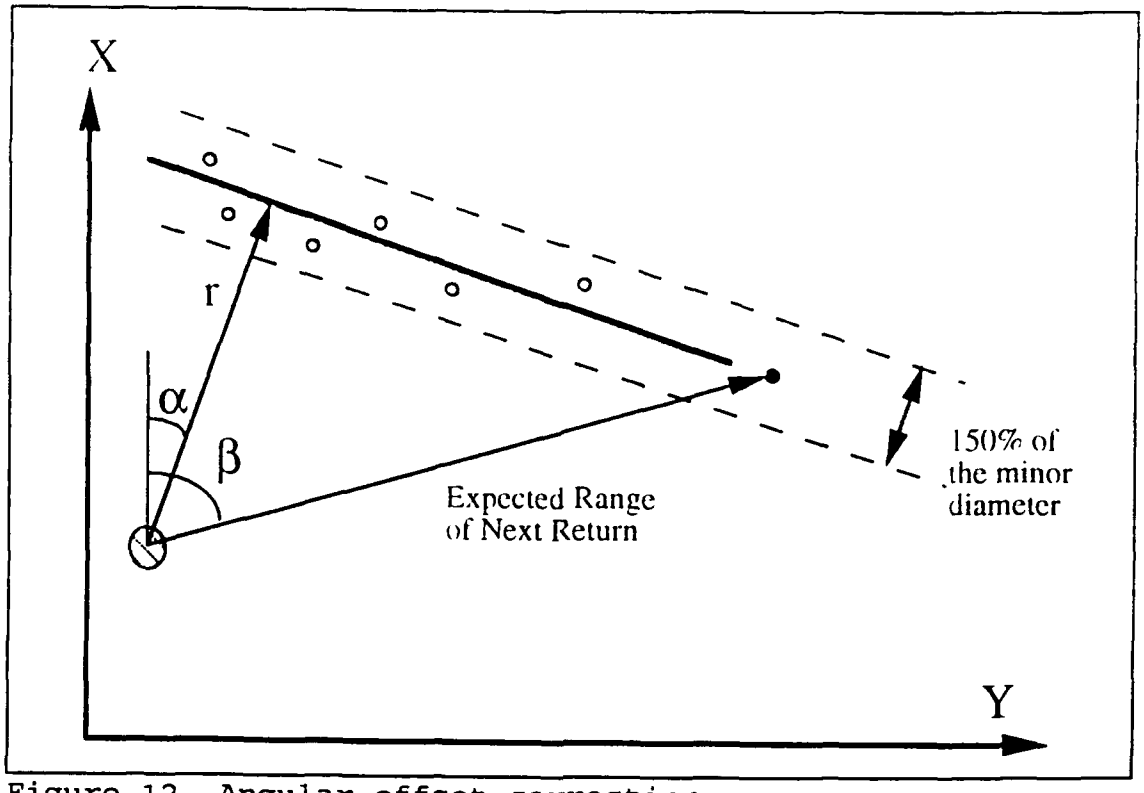

Figure 12. Angular offset correction

declared valid and accepted, and it is added to the batch of points used to update the regression. If the actual range falls outside the minor diameter corrected for angular offset, then it is designated as an *outlier* and saved in a buffer. Each point in succession is evaluated using this criteria.

If only one or two successive outliers occur in a line segment, then they are repositioned to their expected range at that bearing when the next valid point is accepted. If three outliers occur in a row, then they are considered to be a new line segment and the old line segment is terminated. This criteria is based on an extensive review of sonar data files

which showed that the sonar occasionally generates spurious ranges, but they never occur at three successive bearings.

## D. KEY FEATURE IDENTIFICATION

Once the linear regression algorithm has generated a line segment, key points can be identified at the beginning and ending of each line segment. In this thesis it has been decided that key points must meet one of two criteria. First, when the end of one line segment coincides with the beginning of the next line segment, then that point is designated as a key point. For example, this criteria is satisfied at the corners of the hovering tank. Second, when the beginning point of a new line segment has a range that is less than the range to the end of the previous segment, then the new line segment beginning point is designated as a key point. Similarly, when the range to the end of an old line segment is less than the range to the beginning of the new line segment, then the ending point of the old line segment is designated as a key point. The beginning and ending points of line segments which lie behind other segments can not be designated as key points due to the shadowing effects created by the sonar head only accepting the first valid range return. As the vehicle moves through the water, the line segments at greater distances will change as shadowing is unmasked due to the shadowing effect. For example, this criteria is necessary to

distinguish the ends of the cylindrical sonar targets located in the hovering tank.

## E. DETERMINATION OF VEHICLE RELATIVE POSITION AND HEADING

Reliable identification of key points allows for the determination of vehicle relative position and heading.

### 1. Vehicle Relative Position

Each time a key point is designated, the relative position of the key point to the vehicle is known from the sonar return at that bearing. If the position of the key point is known, the global position of the vehicle can be determined using the coordinate transformation. Alternatively, if no global positions are known, the vehicle can still navigate within its perceived environment based only on its relative position to key points.

### 2. Vehicle Heading

Vehicle heading ($\psi$) can be determined from the perceived scene only if the orientation of an object in the perceived scene is known. For example, the walls of the hovering tank coincide with the global hovering tank coordinate system. It follows that the true heading of the vehicle can be determined by adding the known orientation angle of a wall with the wall's $\alpha$ as determined by the regression analysis.

# V. RESULTS

## A. GENERAL

A series of static performance tests were conducted in the NPS hovering tank with the ST1000 sonar system. Results presented here include use of the ST1000 sonar in the scanning and profiling modes. Regression analysis parameters are presented showing the precision with which the sonar can represent its perceived scene. Finally, results of the regression analysis applied to an actual set of data are presented.

## B. ST1000 SONAR SCANNING MODE

A representation of the video display with the sonar operating in the scanning mode is shown in Figure 13. Darker colors represent strong returns while lighter colors represent relatively weak returns. In this case the gain has been adjusted to an optimum level of 15. Figure 14 depicts the sonar operating at a much higher gain. Some degradation of the picture results due to the increased number of noise returns generated by the higher gain.

Figure 15 illustrates the use of sector scanning. In particular, a 90 degree sector centered about a bearing of 075 degrees is being scanned by the sonar.

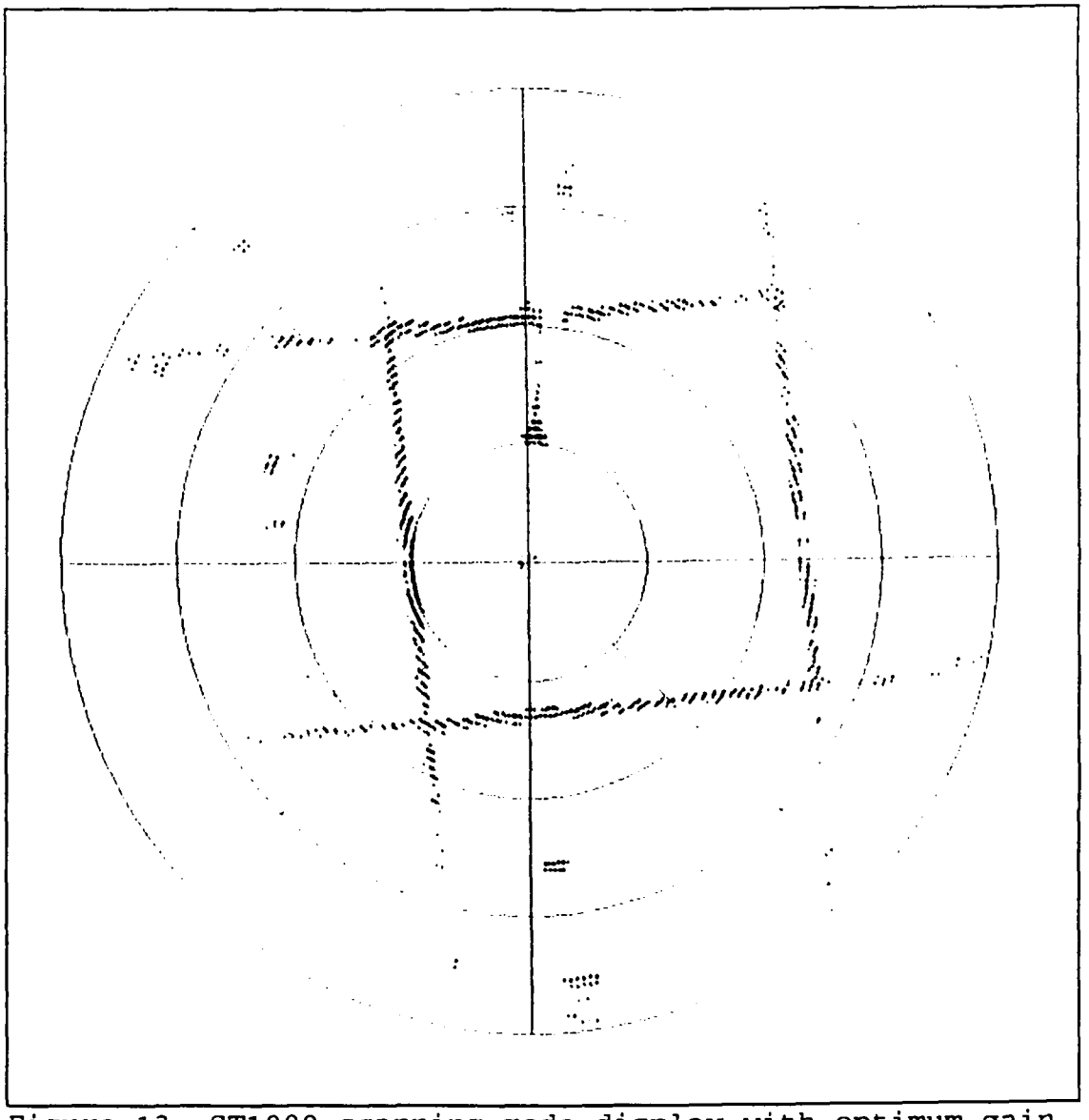

Figure 13. ST1000 scanning mode display with optimum gain

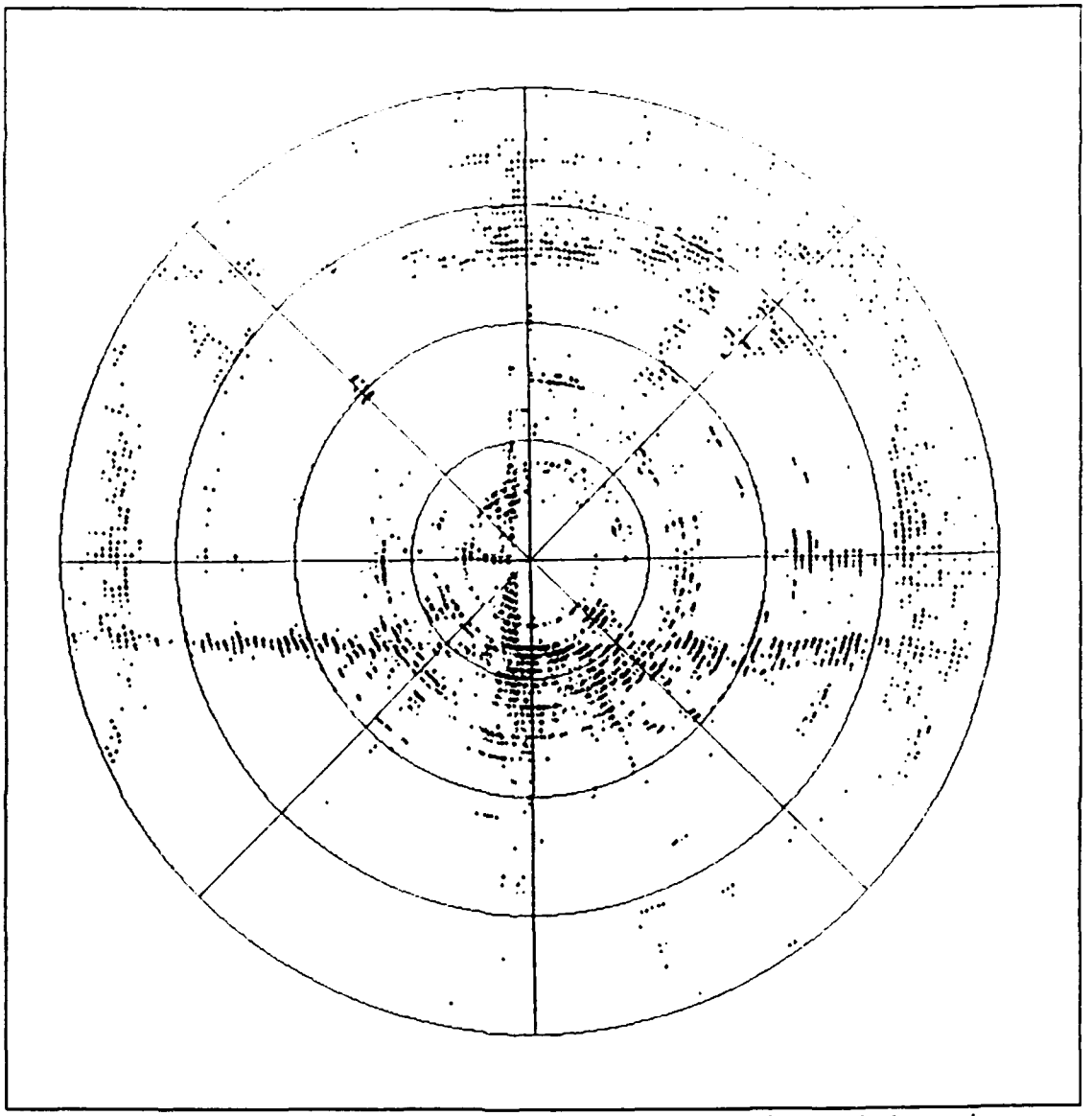

Figure 14. ST1000 scanning mode display with high gain

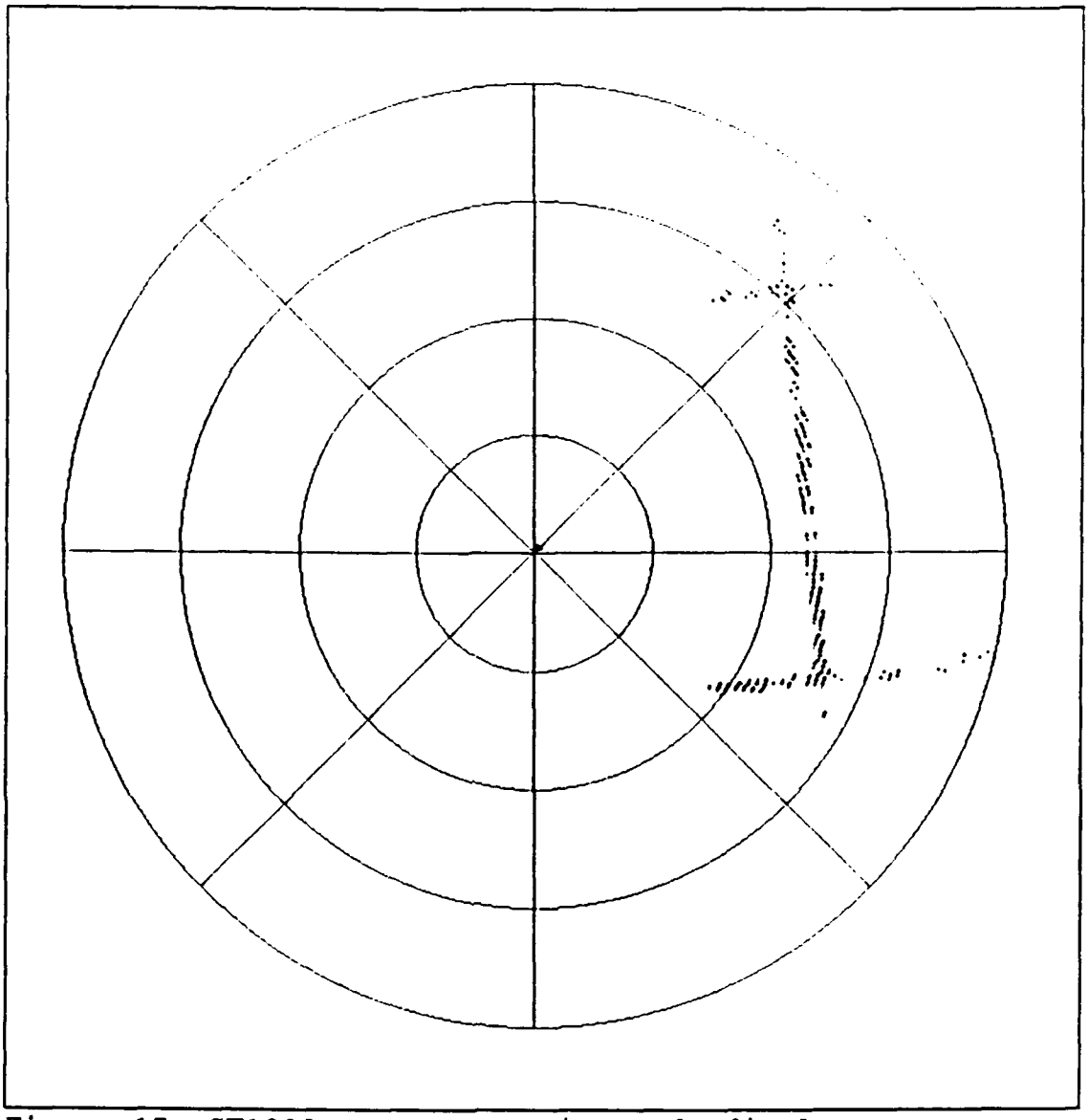

Figure 15. ST1000 sector scanning mode display

## C. ST1000 PROFILING MODE

### 1. Regression Analysis Parameters

Results from a set of 50 sonar returns along a known straight wall measured at a range of 2 meters in the NPS hovering tank are presented. The regression analysis was started with only three points and the values of major diameter, minor diameter, and ellipse thinness ratio ($\rho$) were determined as each point was added to the regression.

#### *a. Major Diameter*

Figure 16 shows the behavior of the major diameter as the number of sonar returns increases. As expected, the major diameter increases linearly as additional data points are accepted along a straight line.

#### *b. Minor Diameter*

Figure 17 shows the behavior of the minor diameter as the number of sonar returns increases. The minor diameter consistantly measured between 2 and 4 centimeters along the wall. This represents an absolute minimal amount of data scatter and provides an indication of the precision of the segment identification as $\pm$ 2 centimeters. At a range of 2 meters this is an error of only 1 percent.

#### *c. Ellipse Thinness Ratio ($\rho$)*

Figure 18 shows the behavior of the ellipse thinness ratio as the number of sonar returns increases. The ellipse thinness ratio drops drastically as the number of data

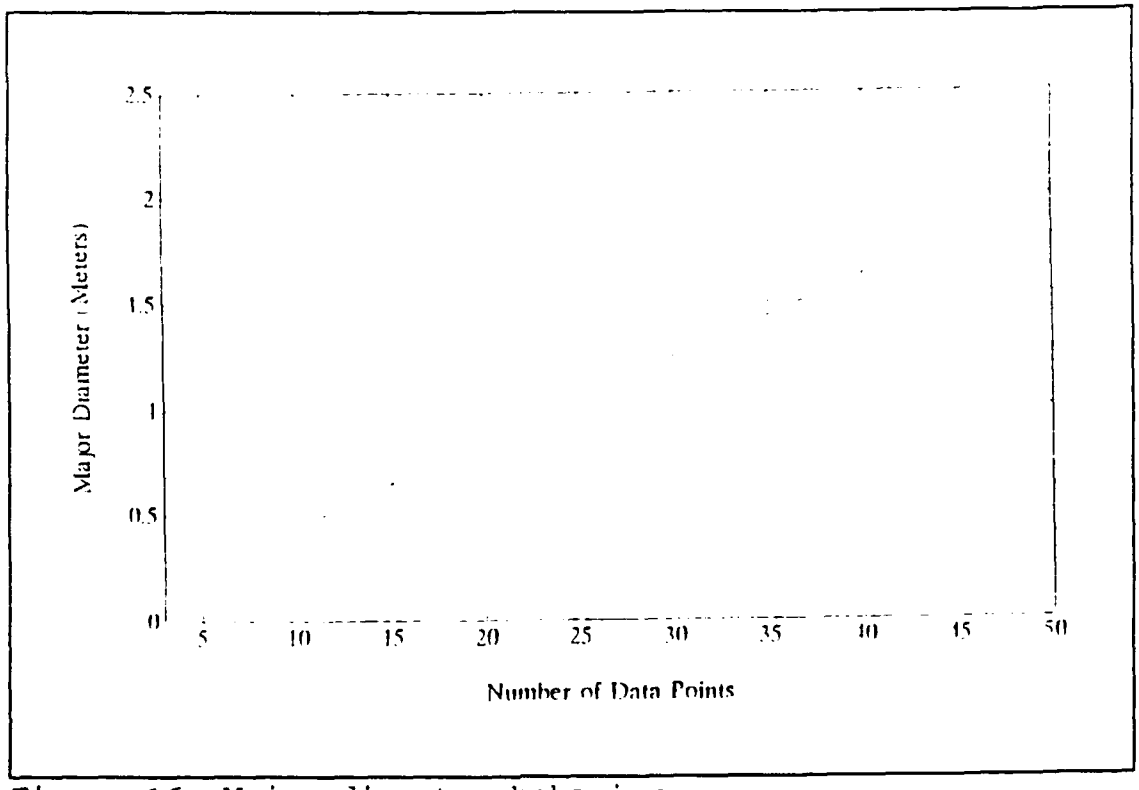

Figure 16. Major diameter behavior

points increases from 3 to 10. A $\rho$ of 0.1 has been selected as the criteria to ensure a feature is linear, and this led to the initial use of 6 data points in the regression analysis. A final value of $\rho$ = 0.02 indicates the outstanding precision with which the ST1000 profiling sonar and the regression analysis can represent linear features.

**2. Regression Analysis Application**

The linear regression algorithm was applied to numerous sets of data. One particular case is presented here showing the results at each stage of the regression analysis, along with the images developed for several sets of sonar data.

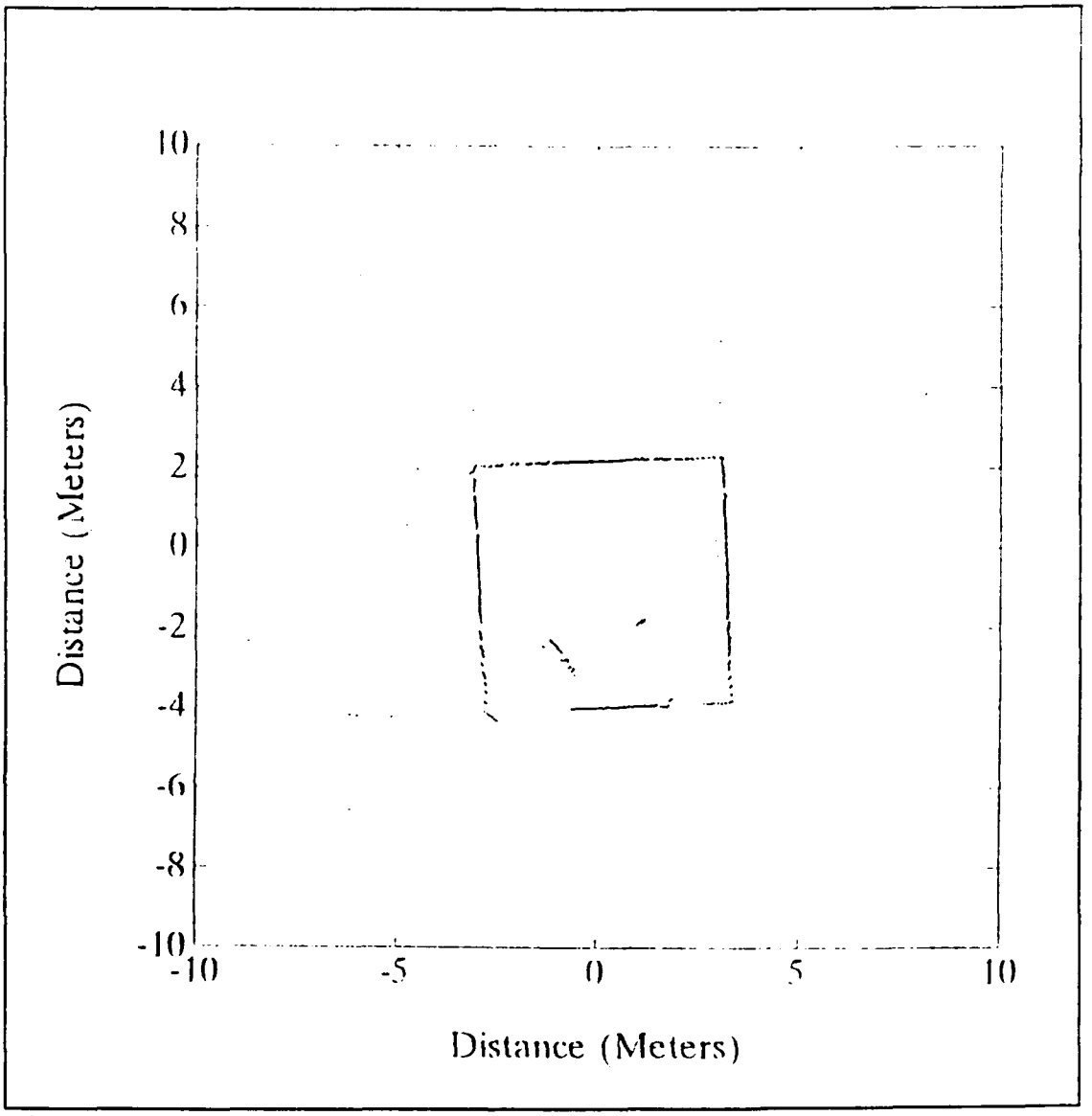

Figure 19. Raw sonar data returns

(·) with the relative position of the sonar to the key points being shown as the X. The actual values of the parametric representation $r$ and $\alpha$, as well as the major diameter, for each line segment are listed in Table 1 and coincide with the line segments shown in Figure 22.

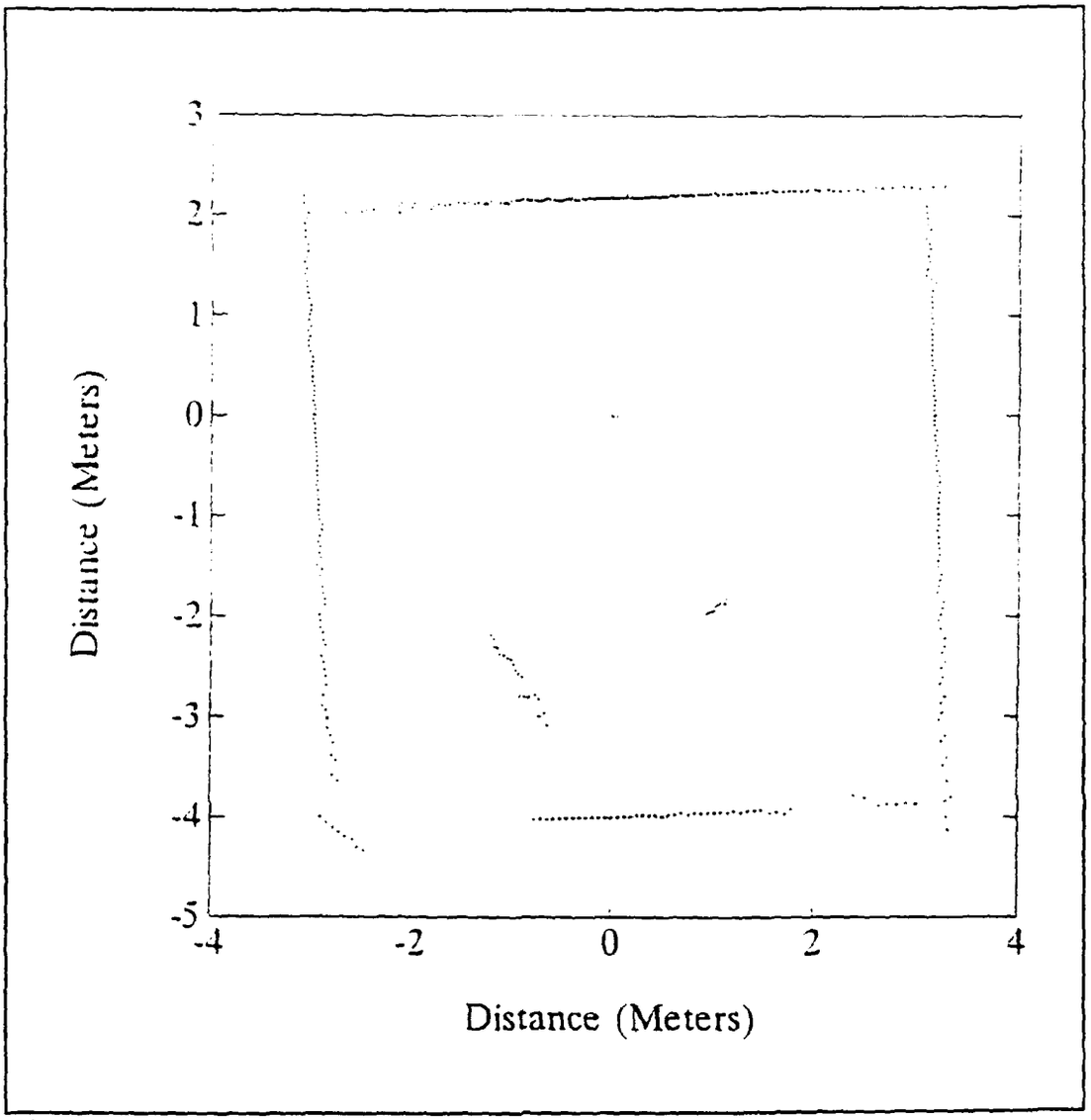


Figure 20. Post processed sonar data

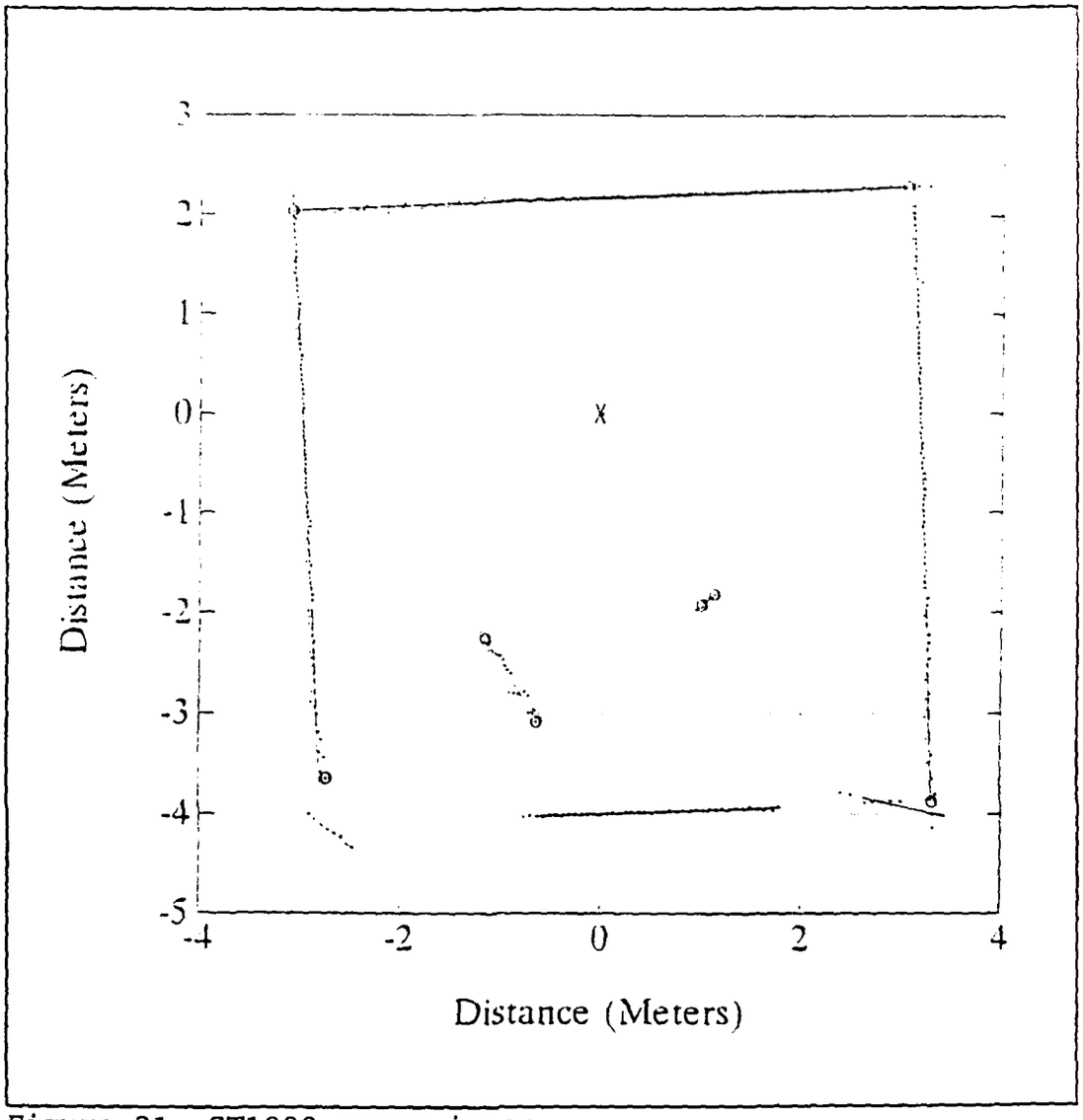


Figure 21. ST1000 sonar image

**TABLE I. ACTUAL VALUES OF PARAMETRIC REGRESSION PARAMETERS**

| Segment | $r$ (Meters) | $\alpha$ (Degrees) | Major Diameter (Meters) |
|---|---|---|---|
| 1 | 2.1692 | -2.1992 | 3.6311 |
| 2 | 3.1797 | 88.0945 | 6.8457 |
| 3 | 3.1515 | -167.0455 | 1.3064 |
| 4 | 2.1344 | 144.9227 | 0.3168 |
| 5 | 3.9996 | 177.9344 | 2.9828 |
| 6 | 2.2060 | -123.0220 | 1.2599 |
| 7 | 4.9574 | -142.4918 | 0.7192 |
| 8 | 2.9876 | -92.8467 | 6.2736 |
| 9 | 2.1699 | -2.5221 | 3.6583 |

It is interesting to note the length of the horizontal cylinder measured by the sonar as the major diameter of segment 6 is 1.2599 meters. This is quite close to the actual length of 1.01 meters. The difference is attributed to the aspect of the sonar beam impinging on the end of the cylinder as well as the effect of the sonar beam width.

Addition of the parameter $r$ between the opposite walls provides the dimensions of the hovering tank as 6.169 by 6.167 meters. This leads to an average error of only 7 centimeters on a 6 meter range scale when compared with the measured dimensions of the hovering tank of 6.096 by 6.096 meters (20 by 20 feet).

An additional image generated by the sonar and regression algorithm is shown in Figure 23.

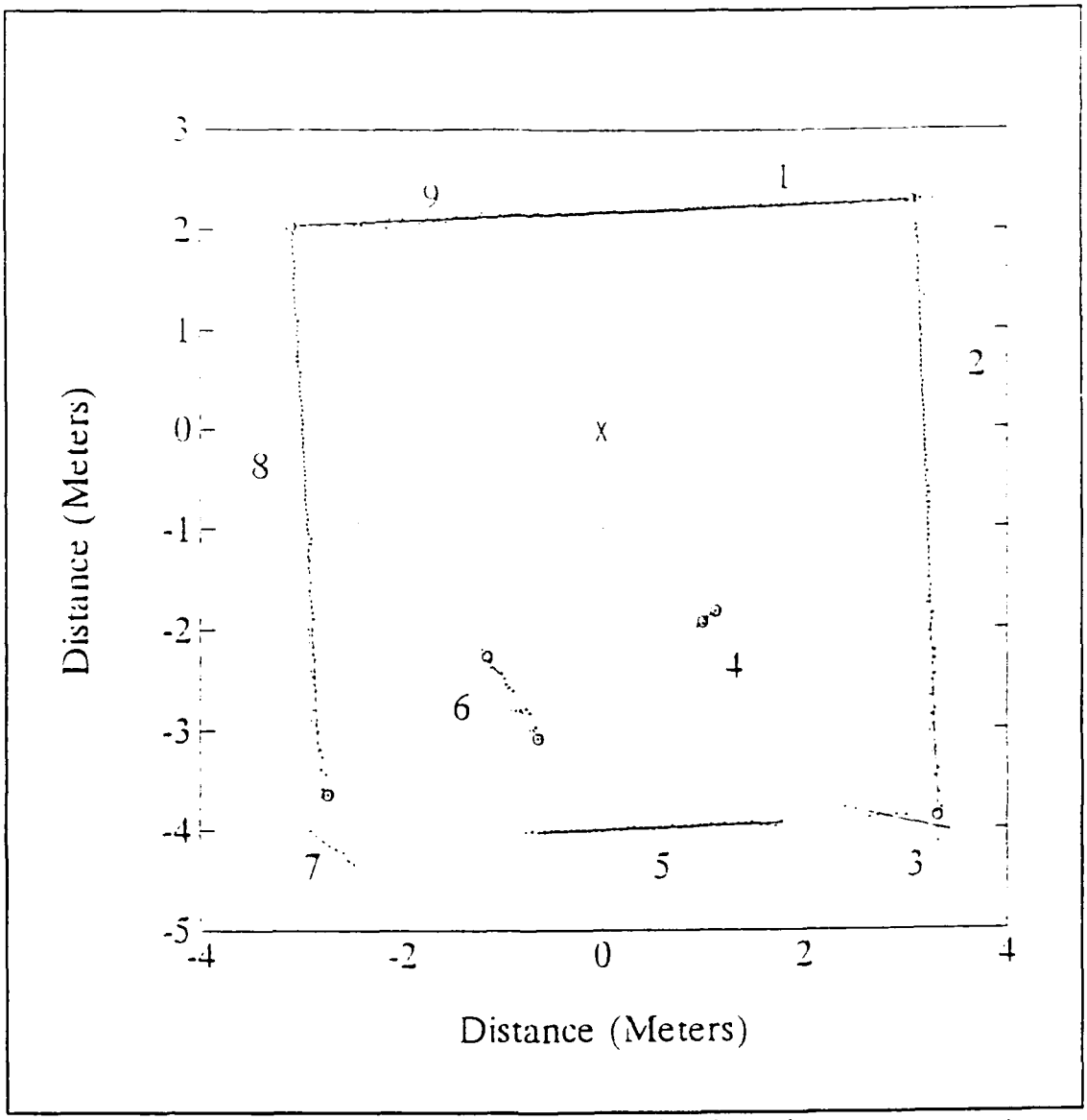


Figure 22. ST1000 sonar image identifying image segments

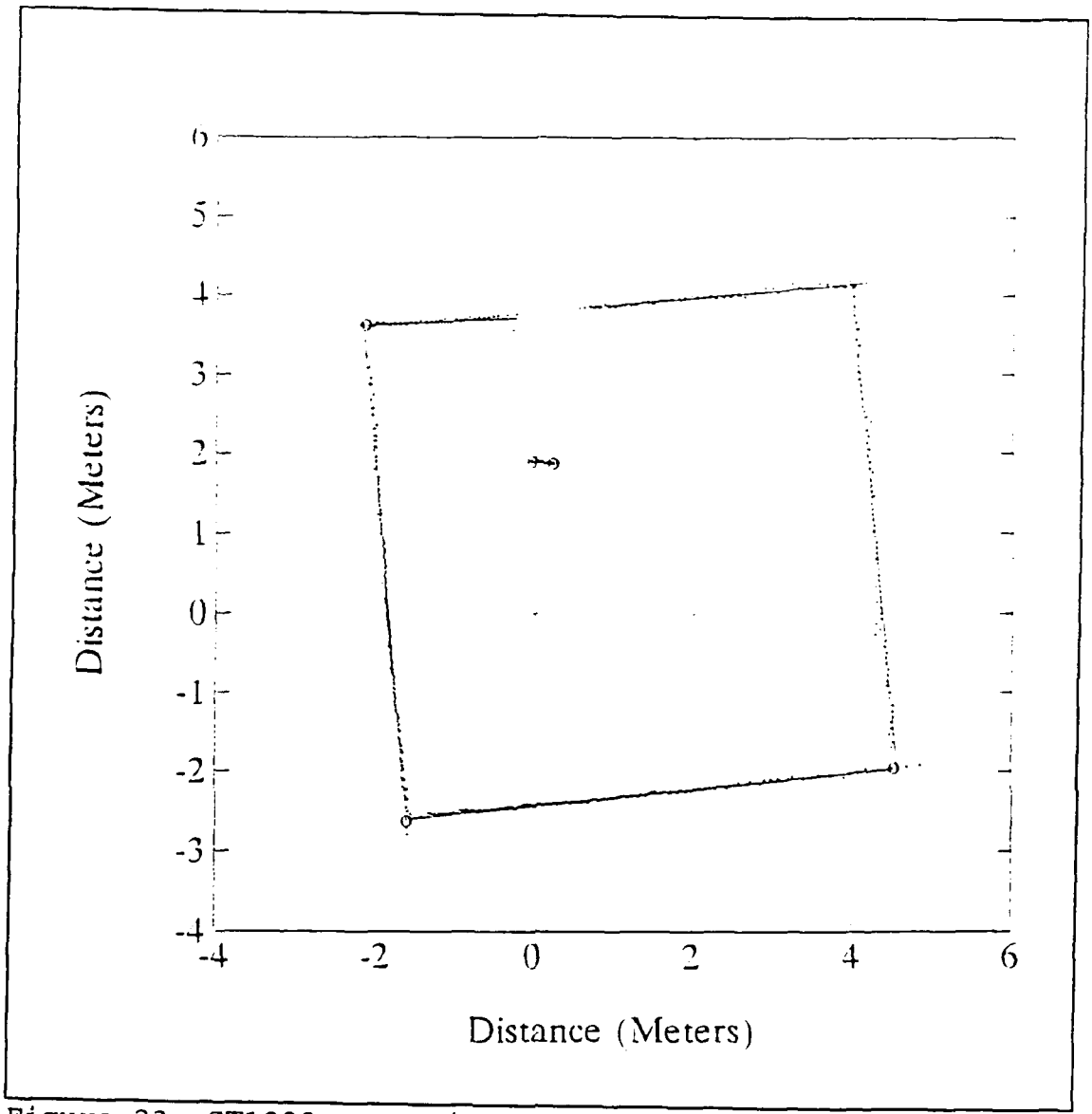


Figure 23. ST1000 sonar image

# VI. CONCLUSIONS AND RECOMMENDATIONS

## A. CONCLUSIONS

Based on the results obtained from the static performance analysis of the Tritech ST1000 sonar system the following conclusions can be made:

- The operating characteristics of the Tritech ST1000 sonar system are ideally suited for object localization on an AUV,
- The use of a linear regression analysis and evaluation of the equivalent ellipse of inertia minor diameter provides a satisfactory criteria for accepting valid sonar returns,
- Images can be successfully developed and key points identified with a precision that is with 1 percent of range.

## B. RECOMMENDATIONS

While a static performance analysis of the Tritech ST1000 sonar system has provided much insight into its capabilities, it is recommended to:

- Evaluate the required computer capability necessary to implement the linear feature extraction algorithm and determine if it can be done recursively as opposed to batch processing, within the constraints of a real time controller on NPS AUV II.
- Add a time factor to the algorithm to include the effects of vehicle motion.
- Analyze the use of a similar sonar system that has a larger beam width such that the sonar will have a viable search capability.

- Develop an algorithm that will automatically determine and adjust the sonar to the proper gain settings for the environment in which it is operating.

- Continue to develop the ability for NPS AUV II to autonomously control the sonar system as required in order to search for, identify, and locate objects.

## APPENDIX A

MATLAB COMPUTER CODE FOR LINEAR FEATURE EXTRACTION
AND KEY POINT IDENTIFICATION

```
*****Load data file for processing*****
load SCANLINE_PRF_L27.D;
BRGACT = SCANLINE_PRF_L27(:,2);
RNGACT = SCANLINE_PRF_L27(:,3);

*****Initialize counter values*****
a = 639;      *****Initial data point*****
b = a + 5;    *****End point of initial line segment*****
e = 0;        *****Counter for outliers*****
j = 1;        *****Counter for line segments*****
k = 1;        *****Counter for key points*****

*****Set up loop to desired length of data set*****
while b<= 1045;
    RNG(b) = RNGACT(b);

    *****Initialize Moments*****
    m10 = 0.0;
    m01 = 0.0;
    m11 = 0.0;
    m20 = 0.0;
    m02 = 0.0;

    *****Loop to incrementally calculate moments*****
    for i=a:b;
        BRGRAD(i) = BRGACT(i)*pi/180; **Convert to radians**

        *****Reposition outliers to expected values*****
        if i == b;
            if e == 2;
                RNGACT(b-1) = REXP(b-1);
                RNGACT(b) = REXP(b);
            elseif e == 1;
                RNGACT(b) = REXP(b);
            else;
            end;
        end;
```

```
     ***Calculate X and Y positions of raw data points***
     XP(i) = RNGACT(i)*cos(BRGRAD(i));
     YP(i) = RNGACT(i)*sin(BRGRAD(i));
     X(i) = RNGACT(i)*cos(BRGRAD(i));
     Y(i) = RNGACT(i)*sin(BRGRAD(i));

     *****Calculate moments*****
     m00 = (b-a)+1;
     m10 = m10 + X(i);
     m01 = m01 + Y(i);
     m11 = m11 + X(i)*Y(i);
     m20 = m20 + X(i)^2;
     m02 = m02 + Y(i)^2;
end;

*****Calculate Secondary moments*****
M20 = m20 - (m10)^2/m00;
M11 = m11 - ((m10*m01)/m00);
M02 = m02 - (m01)^2/m00;

*****Calculate R and α*****
ALPHA(j) = (atan2(-2*M11,M02-M20))/2;
R(j) = (m10/m00)*cos(ALPHA(j))+(m01/m00)*sin(ALPHA(j));

*****Convert to ensure R>0 and -180<α<180*****
if ALPHA(j)*R(j) > 0.0;
     if R(j) < 0.0;
          R(j) = -1.0*R(j);
     end;
     if ALPHA(j) < 0.0;
          ALPHA(j) = pi + ALPHA(j);
     end;
elseif ALPHA(j)*R(j) <= 0.0;
     if R(J) < 0.0;
          R(j) = -1.0*R(j);
     end;
     if ALPHA(j) > 0.0;
          ALPHA(j) = ALPHA(j) - pi;
     end;
end;

*****Calculate major and minor moments*****
Major(j)=(M20+M02)/2+sqrt(((M02-M20)^2)/4+(M11)^2);
Minor(j)=(M20+M02)/2-sqrt(((M02-M20)^2)/4+(M11)^2);

*****Calculate major and minor diameters*****
dmajor(j) = 4*sqrt(Major(j)/m00);
dminor(j) = 4*sqrt(Minor(j)/m00);
```

```
*****Calculate ellipse thinness ratio*****

rho(j) = dminor(j)/dmajor(j);

*****Set segment start point based on raw data*****
sx(j) = X(a);
sy(j) = Y(a);

*****Set segment start point based on R and α*****
X1(k)=R(j)/cos(BRGRAD(a)-ALPHA(j))*cos(BRGRAD(a));
Y1(k)=R(j)/cos(BRGRAD(a)-ALPHA(j))*sin(BRGRAD(a));

****Calculate next point expected range and bearing*****
BRGRAD(b+1) = BRGACT(b+1)*pi/180;
g(j)=cos(BRGRAD(b+1)-ALPHA(j));  **angle correction**
REXP(b+1) = abs(R(j)/g(j));

*****Test to evaluate if next point is an outlier*****
if abs(RNGACT(b+1)-REXP(b+1))>abs(0.75*dminor(j)/g(j));
    e = e + 1;    ****Increment the outlier counter****
else;

    *****Reposition ouliers to expected positions*****
    if e == 2;
        RNGACT(b-1) = REXP(b-1);
        RNGACT(b) = REXP(b);
    elseif e == 1;
        RNGACT(b) = REXP(b);
    else;
    end;
    e = 0;   *****Reset outlier counter*****
end;

****Line segment ending and key point identification***
if e == 3;

    *****Set segment end point based on raw data*****
    fx(j) = X(b-2);
    fy(j) = Y(b-2);

    *****Set segment end point based on R and α*****
  X2(k)=R(j)/cos(BRGRAD(b-2)-ALPHA(j))*cos(BRGRAD(b-2));
  Y2(k)=R(j)/cos(BRGRAD(b-2)-ALPHA(j))*sin(BRGRAD(b-2));

    ***For coincident ending and next starting points***
    if abs(RNG(b-1)-RNG(b-2)) < 0.15;
```

```
        *****Designate key points based on raw data*****
        KEYRNG(k) = RNGACT(b-2);
        KEYBRG(k) = BRGRAD(b-2);
        XKEY(k) = X(b-2);
        YKEY(k) = Y(b-2);

        *****Designate key points based on R and α*****
        XKEY2(k) = X2(k);
        YKEY2(k) = Y2(k);


        *****Position based on raw data key point*****
        XPOS(k) = X(b-2)-KEYRNG(k)*cos(KEYBRG(k));
        YPOS(K) = Y(b-2)-KEYRNG(k)*sin(KEYBRG(k));
        k = k + 1;  ****Increnent key point counter****
        a = b - 2;  ****Reset 'a' for next segment****
    else;

        ***For non-coincident ending and start points***
        if (RNGACT(b)-RNGACT(b+1)) > 0.15;

            ***Designate key points based on raw data***
            KEYRNG(k) = RNGACT(b+1);
            KEYBRG(k) = BRGRAD(b+1);
            X(b+1) = RNGACT(b+1)*cos(BRGRAD(b+1));
            Y(b+1) = RNGACT(b+1)*sin(BRGRAD(b+1));
            XKEY(k) = X(b+1);
            YKEY(k) = Y(b+1);

            ***Designate key points based on R and α***
            XKEY2(k) = X(b+1);
            YKEY2(k) = Y(b+1);

            ***Position based on raw data key points***
            XPOS(k) = X(b+1) - KEYRNG(k)*cos(KEYBRG(k));
            YPOS(k) = Y(b+1) - KEYRNG(k)*sin(KEYBRG(k));
        else;

            ***Designate key points based on raw data***
            KEYRNG(k) = RNGACT(b-2);
            KEYBRG(k) = BRGRAD(b-2);
            XKEY(k) = X(b-2);
            YKEY(k) = Y(b-2);

            ***Designate key points based on R and α***
            XKEY2(k) = X2(k);
            YKEY2(k) = Y2(k);

            ***Position based on raw data key points***
            XPOS(k) = X(b-2) - KEYRNG(k)*cos(KEYBRG(k));
            YPOS(k) = Y(b-2) - KEYRNG(k)*sin(KEYBRG(k));
```

```
            end;
            k = k + 1;  ****Increment key point counter****
            a = b + 1;  *****Reset 'a' for next segment*****
        end;
        b = a + 5;  *****Reset 'b' for next segment*****
        j = j + 1;  *****Increment line segment counter*****
        e = 0;      *****Reset the outlier counter*****
    elseif e == 2;

        ****Segment end point for two outliers; raw data****
        fx(j) = X(b-1);
        fy(j) = Y(b-1);

        ****Segment end point for two outliers; R and α****
       X2(k)=R(j)/cos(BRGRAD(b-1)-ALPHA(j)*cos(BRGRAD(b-1));
       Y2(k)=R(j)/cos(BRGRAD(b-1)-ALPHA(j)*sin(BRGRAD(b-1));
        b = b + 1;   ***Increment 'b', accept valid point***
    else;

        ***Segment end point for one/no outliers; raw data**
        fx(j) = X(b);
        fy(j) = Y(b);

        ***Segment end point for one/no outliers; R and α***
        X2(k)=R(j)/cos(BRGRAD(b)-ALPHA(j))*cos(BRGRAD(b));
        Y2(k)=R(j)/cos(BRGRAD(b)-ALPHA(j))*sin(BRGRAD(b));
        b = b + 1;  ***Increment 'b', accaept valid point***
    end;
end;

x=[sx;fx];
y=[sy;fy];
x1=[XKEY1;XKEY2];
y1=[YKEY1;YKEY2];
```

## LIST OF REFERENCES


1. Bane, G., Ferguson, J., "The Evolutionary Development of the Military Autonomous Underwater Vehicle," *Proceedings of the Fifth International Symposium on Unmanned Untethered Technology*, University of New Hampshire, Durham, NH, pp. 60-88, June 1987.

2. Wang, F., "Offshore Oil and Gas Field Development and Applications of Underwater Autonomous Vehicles," *Proceedings of the Third International Symposium on Unmanned Untethered Technology*, University of New Hampshire, Durham, NH, pp. 231-241, June 1983.

3. Thomas, B., "Potential Applications of Autonomous Underwater Vehicles," *Proceedings of the Third International Symposium on Unmanned Untethered Technology*, Durham, NH, pp. 223-225, June 1983.

4. Krabach, M., "Potential AUV Applications to Nuclear Power Plant Inspection," *Proceedings of the Third International Symposium on Unmanned Untethered Technology*, Durham, NH, pp. 226-230, June 1983.

5. Ballard, R., *The Discovery of the Titanic*, pp. 53-58, Warner Books Inc., 1987.

6. Rosenblum, L., Kamgar-Parsi, B., "3-D Reconstruction of Small Underwater Objects Using High-Resolution Sonar Data," *Proceedings of the 1992 Symposium on Autonomous Underwater Vehicle Technology*, Washington, DC, pp. 228-235, June 1992.

7. Elfes, A., "Sonar-Based Real World Mapping and Navigation," *IEEE Journal of Robotics and Automation*, vol. RA-3, no. 3, pp. 249-265, 1987.

8. Bahl, R., "Object Classification Using Compact Sector-Scanning Sonars in Turbid Waters," *Proceedings of the International Advanced Robotics Programme 1st Workshop on Mobile Robots for Subsea Environments*, Monterey, CA, pp. 81-95, October 1990.

9. Gordon, A., "Use of Laser Scanning System on Mobile Underwater Platforms," *Proceedings of the 1992 Symposium on Autonomous Underwater Vehicle Technology*, Washington, DC, pp. 202-205, June 1992.

10. Chu, J., Lieberman, L., Downes, P., "Automatic Camera Control for AUVs: A Comparison of Image Assessment Methods," *Proceedings of the 1992 Symposium on Autonomous Underwater Vehicle Technology*, Washington, DC, pp. 191-201, June 1992.

11. Lane, D., "The Investigation of a Knowledge Based System Architecture in the Context of a Subsea Robotic Application," Ph.D. Dissertation, Heriot-Watt University, Edinburgh, 1986.

12. Russell, G., Lane, D., "A Knowledge Based System Framework for Environmental Perception in a Subsea Robotic Context," *IEEE Journal of Ocean Engineering*, July 1986.

13. Russell, G., Lane, D., "An Intelligent Guidance System Utilizing Sector Scan Sonar Image Interpretation," *Proceedings of the Fourth International Symposium on Unmanned Untethered Technology*, University of New Hampshire, Durham, NH, pp. 257-271, June 1985.

14. Kanayama, Y., Floyd, C., "Underwater Obstacle Recognition Using a Low-Resolution Sonar," *Proceedings of the Seventh International Symposium on Unmanned Untethered Technology*, University of New Hampshire, Durham, NH, pp. 309-327, September 1991.

15. Kinsler, L., Frey, A., Coppens, A., Sanders, J., *Fundamentals of Accoustics*, pp. 397-399, John Wiley and Sons Inc., 1982.

16. Kwak, S., McGhee, R., Bihari, T., "Rational Behavior Model: A Tri-Level Multiple Paradigm Architecture for Robot Vehicle Control Software," Naval Postgraduate School Department of Computer Science *Technical Report NPSCS-92-003*, March 1992.

17. Brutzman, D., "NPS AUV Integrated Simulator," Master's Thesis, Naval Postgraduate School, Monterey, CA, March 1992.

18. Roberts, L., "Machine Perception of Three-Dimensional Solids," *Optical and Electro-Optical Information Processing*, pp. 159-197, MIT Press, 1965.

19. Kanayama, Y., Noguchi, T., "Spatial Learing by an Autonomous Mobile Robot with Ultrasonic Sensors," University of California Santa Barbara Department of Computer Science *Technical Report TRCS89-06*, February 1989.

## INITIAL DISTRIBUTION LIST

| | | |
|---|---|---|
| 1. | Defense Technical Information Center<br>Cameron Station<br>Alexandria, VA 22304-6145 | 2 |
| 2. | Library, Code 0142<br>Naval Postgraduate School<br>Monterey, CA 93943-5000 | 2 |
| 3. | Dr. Matthew D. Kelleher<br>Code ME/Kk<br>Chairman, Mechanical Engineering Department<br>Naval Postgraduate School<br>Monterey, CA 93943-5000 | 1 |
| 4. | Curricular Office, Code 34<br>Naval Postgraduate School<br>Monterey, CA 93943-5000 | 1 |
| 5. | Dr. Anthony J. Healey<br>Code ME/Hy<br>Mechanical Engineering Department<br>Naval Postgraduate School<br>Monterey, CA 93943-5000 | 1 |
| 6. | Lt Barry W. Ingold<br>Naval Submarine School<br>Code 81, SOAC Class 93040<br>Box 700<br>Groton, CT 06349-5700 | 1 |
| 7. | Mr. Gary Trimble<br>Lockheed Marine Systems Division<br>P.O. Box 3504<br>Sunnyvale, CA 94088-3504 | 1 |
| 8. | Dr. Jim Bellingham<br>MIT Sea Grant Program<br>MIT<br>Cambridge, MA 02139 | 1 |

9. Albert J. Faulstich/Dan Steiger — 1
Office of Naval Technology
Code ONT-23
800 North Quincy St.
Arlington, VA 22217

10. Chris Agoras/Chris Hellebaum — 1
Naval Underwater Systems Center (NUSC)
Newport, RI 02841-5047

11. Mr. Richard Blidberg — 1
University of New Hampshire
Marine Systems Lab
Durham, NH 03824

12. Dr. Dana Yoerger — 1
Woods Hole Oceanographic Institution
Deep Submergence Laboratory
Woods Hole, MA 02543

13. Mr. Mike Lee — 1
MBARI
160 Central Ave.
Pacific Grove, CA 93950